

Final Technical Report for

Department of Energy Award DE-FE0031988

**Title: *Developing a Facile Technology for Converting Domestic US Coal into High-Value Graphene***

**Awarded Under: DE-FOA-0002185 - *Coal-Derived Materials for Building, Infrastructure, and Other Applications* - Area of Interest 3 - *Coal-Derived High-Value Carbon Products***

**Sponsoring Program Office: Office of Fossil Energy and Carbon Management**

**Name of Recipient: Universal Matter, Ltd.**

**900 South Loop West; Suite 175**

**Houston, Texas, USA 77054**

**DUNS #: 117195704**

**UEI #: QK47YVM5ELL9**

**Principal Investigator: Duy Luong ([duyxl@universalmatter.com](mailto:duyxl@universalmatter.com) or 832-727-8212)**

**Business Contact: Dru Kefalos ([druk@universalmatter.com](mailto:druk@universalmatter.com) or 512-667-4450)**

**Team members: University of Missouri (Columbia, Missouri, USA)**

**Award Period of Performance: April 1, 2021 – February 28, 2023**

## Table of Contents

|  |    |
|--|----|
| List of Figures .....  | 1  |
| List of Tables .....   | 2  |
| Acknowledgement .....  | 4  |
| Disclaimer .....   | 4  |
| Summary .....  | 5  |
| Introduction .....   | 6  |
| Development of Flash Joule Heating Systems .....                                 | 6  |
| Further Development of Flash Joule Heating Systems .....                         | 11 |
| Flash Joule Heating of Bituminous Coal .....                                     | 13 |
| Flash Joule Heating of Metallurgical Coke .....                                  | 14 |
| Flash Joule Heating of Anthracite Coal .....                                     | 16 |
| Scale up of the Flash Joule Heating process: Achievements and challenges .....   | 19 |
| Development of a machine learning method for process optimization .....          | 22 |
| Statistical modeling .....   | 23 |
| Evaluation of graphene in different applications .....                           | 26 |
| Development of method to disperse metallurgical coke turbostratic graphene ..... | 26 |
| Flash graphene in concrete .....   | 28 |
| Flash graphene in asphalt .....  | 30 |
| Flash graphene in epoxy/coatings .....   | 33 |
| Technoeconomic analysis .....  | 35 |
| Technology Gap Assessment (TGA) .....  | 37 |
| Bibliography and References .....  | 38 |

## List of Figures

|   |    |
|---|----|
| <b>Figure 1.</b> Flash Joule Heating system at Universal Matter's Houston Innovation Center .....   | 7  |
| <b>Figure 2.</b> Prototype AC Flash Joule Heating system .....  | 8  |
| <b>Figure 3.</b> Circuit diagram of the high-power AC Flash Joule Heating system .....  | 8  |
| <b>Figure 4.</b> Electrical profile (current vs. time) of the Flash Joule Heating of 20 g of metallurgical coke .....   | 9  |
| <b>Figure 6.</b> New Flash Joule Heating tool .....   | 10 |
| <b>Figure 5.</b> Electrical schematic of the new Flash Joule Heating tool .....   | 10 |
| <b>Figure 7.</b> Flash Joule Heating chamber at Universal Matter's Houston Innovation Center .....  | 12 |
| <b>Figure 8.</b> Layout of new Flash Joule Heating reactor constructed of refractory bricks .....   | 12 |
| <b>Figure 9.</b> Raman spectrum of graphene obtained from Flash Joule Heating of metallurgical coke in the refractory brick Flash Joule Heating reactor ..... | 13 |

|  |    |
|--|----|
| <b>Figure 10.</b> Current (a) and temperature (b) profiles vs. time of a DC flash (a) vs. a PWM flash (b). Note: The pulse sequence of the PWM flash is shown in the inset.....  | 14 |
| <b>Figure 11.</b> XRD (a) and Raman spectra (b) of turbostratic graphene synthesized from the Flash Joule Heating of metallurgical coke.....   | 15 |
| <b>Figure 12.</b> Raman spectra of MCTG synthesized from DC and AC Flash Joule Heating.....  | 15 |
| <b>Figure 13.</b> TEM characterization of metallurgical coke derived TG .....  | 16 |
| <b>Figure 14.</b> Raman spectrum of anthracite coal derived TG .....   | 17 |
| <b>Figure 15.</b> Raman spectra of anthracite coal derived flash graphene.....   | 18 |
| <b>Figure 16.</b> Overlayed X-ray diffractograms of anthracite coal and anthracite coal derived FG.....  | 18 |
| <b>Figure 17.</b> SEM image of an anthracite coal derived FG flake.....  | 19 |
| <b>Figure 18.</b> Profile obtained from the Flash Joule Heating of 1.2 kg of MC .....  | 20 |
| <b>Figure 19.</b> Raman spectrum of the product obtained from the Flash Joule Heating of 1.2 kg of MC.....   | 20 |
| <b>Figure 20.</b> Semi-automated Flash Joule Heating reactor with carbon black substrate (left and middle) and graphene product (right) .....  | 21 |
| <b>Figure 22.</b> Sacrificial layer (molding sand) of Flash Joule Heating reactor after experiment.....  | 22 |
| <b>Figure 21.</b> Damage to Flash Joule Heating reactor components resulting from high temperature of Flash Joule Heating experiment .....   | 22 |
| <b>Figure 23.</b> Screenshots from current database tracking app for Flash Joule Heating data and dispersion data.....   | 23 |
| <b>Figure 24.</b> Screenshot of Flash Joule Heating datasets after data cleaning and handling categorical features.....  | 24 |
| <b>Figure 25.</b> Distribution and kernel density estimates plots of the whole dataset .....   | 24 |
| <b>Figure 26.</b> Violin plots of the dataset .....  | 25 |
| <b>Figure 27.</b> Pearson correlation coefficient matrix of the Flash Joule Heating parameters.....  | 25 |
| <b>Figure 28.</b> SEM image of Flash Graphene derived from metallurgical coke .....  | 27 |
| <b>Figure 29.</b> UV-vis absorption for various dispersions (in NMP) of untreated MC-FG, MC-FG after the pyrene milling process ("MC-FG-Pyrene"), and MC-FG after the hydroquinone milling process ("MC-FG-Hydroquinone")..... | 27 |
| <b>Figure 30.</b> SEM and TEM images of MC-FG after the pyrene milling process.....  | 28 |
| <b>Figure 31.</b> SEM and TEM images of MC-FG after the hydroquinone milling process.....  | 28 |
| <b>Figure 32.</b> Chemical structures of pyrene (a) and hydroquinone (b) .....   | 28 |
| Figure 33. Photographs of concrete sample production (left), concrete samples (middle left), and sample testing (middle right, right) .....  | 29 |
| <b>Figure 34.</b> Frequency sweep tests after long-term aging (PAV) of asphalt samples .....   | 30 |
| <b>Figure 35.</b> $T_{c,s}$ - $T_{c,m}$ aging chart for asphalt samples .....  | 31 |
| <b>Figure 36.</b> $\Delta T_c$ of graphene modified asphalt binder compared to base binder and SBS-modified binder   | 32 |
| <b>Figure 37.</b> Intersection of $T_{c,s}$ and $T_{c,m}$ of base asphalt binder, SBS modified binder, and graphene modified binder .....  | 33 |
| <b>Figure 38.</b> Water permeation test of MC-FG improved epoxy coating .....  | 34 |

## List of Tables

|   |    |
|---|----|
| <b>Table 1.</b> Flash Joule Heating parameters obtained for metallurgical coke samples..... | 20 |
|---|----|

|  |    |
|--|----|
| <b>Table 2.</b> Compressive strength results from concrete control samples and MC TG reinforced concrete samples.....    | 29 |
| <b>Table 3.</b> Rheology properties of base asphalt binder, SBS-, and MC-FG- modified binder.....                        | 31 |
| <b>Table 4.</b> Economic summary of the Flash Joule Heating process to convert coal derived feedstocks to graphene ..... | 35 |
| <b>Table 5.</b> Market Projects for Graphene in Coatings, Adhesive, and Lubricants .....                                 | 36 |
| <b>Table 6.</b> Technology Gap Assessment.....   | 37 |

#### Acknowledgement

This material is based upon work supported by the Department of Energy under Award Number DE-FE0031988.

#### Disclaimer

This report was prepared as an account of work sponsored by an agency of the United States Government. Neither the United States Government nor any agency thereof, nor any of their employees, makes any warranty, express or implied, or assumes any legal liability or responsibility for the accuracy, completeness, or usefulness of any information, apparatus, product, or process disclosed, or represents that its use would not infringe privately owned rights. Reference herein to any specific commercial product, process, or service by trade name, trademark, manufacturer, or otherwise does not necessarily constitute or imply its endorsement, recommendation, or favoring by the United States Government or any agency thereof. The views and opinions of authors expressed herein do not necessarily state or reflect those of the United States Government or any agency thereof.

## Summary

### *Developing a Facile Technology for Converting Domestic US Coal into High-Value Graphene*

Universal Matter Ltd. was formed in July 2019 to scale-up and commercialize a breakthrough process, Flash Joule Heating (FJH), to transform different coal grades, into high-quality graphene. This graphene is made using a high-voltage electric discharge that brings the carbon source to temperatures higher than 3,000 K in less than 10 milliseconds. The short burst of electricity breaks all chemical bonds in the feedstock and reorders the carbon atoms into exceptionally thin layers of a special type of graphene, at an estimated \$100 per ton in electricity cost. This process is capable of producing 1-5 layer-thick high-quality graphene (with defects of <0.05% and purity of >99%) in a green, practical, and cost-effective process.

The graphene produced in the FJH process is a very special kind of graphene called “turbostratic graphene” (TG). TG offers superior physical properties compared to other graphene structures on a similar weight basis. Unlike graphene made from graphite using traditional techniques, the graphene layers in TG stack in an irregular pattern that allows the graphene powder to be exfoliated more easily and blend more evenly within other materials. The TG produced using our FJH technology is the most economical graphene product that opens up significant large volume markets for end-use applications; it would allow the use of TG made from coal for commercial applications in several market segments including energy storage, sensors, hyper-lubricants, reinforced plastics, and building materials such as concrete.

Depending on the feedstock and processing parameters used in FJH, different morphologies of graphene can be achieved. The main objective of this project is to optimize the process by using statistical modeling and to validate the technical and economic benefits of producing graphene by using different grades of coal or coal derived materials as the feedstock for FJH process. The graphene products developed from different feedstocks will be studied for application development in different strategic markets to further validate the cost/performance advantages and the environmental benefits that can be realized by the incorporation of graphene-based modifiers into different end-use applications.

## Introduction

In 2010, the Nobel Prize in physics was awarded for leading-edge experiments on a two-dimensional material called graphene [1]. Graphene, a “wonder material”, is comprised of a honeycomb lattice structure of carbon atoms and has shown the potential to generate disruptive technologies. Ever since its discovery, a wide range of impressive properties have been reported for graphene, including high electron mobility of over  $200,000 \text{ cm}^2 \text{ V}^{-1}\text{S}^{-1}$  at electron density of  $\sim 2 \times 10^{11} \text{ cm}^{-2}$  [2], high thermal conductivity of  $\sim 5 \times 10^3 \text{ Wm}^{-1}\text{K}^{-1}$  [3], impermeability to gasses despite being one atom thick [4], optical transparency of 97.7% [5], ballistic transport of electrons [6, 7], and being “the strongest material ever measured” with ultimate tensile strength of 130 GPa and Young’s modulus of 1 TPa [8]. The fact that all of these properties are found within a single material has stimulated great interest in graphene.

Within a mere decade, hundreds of academic institutions and commercial companies are now actively exploring new technology opportunities for transforming key industries such as energy, electronics, and many others by developing a wide spectrum of new high-performance graphene-based nanomaterials. In spite of this, graphene is still only at the early stages of commercial development as a number of challenges need to be addressed. The first of these has been a lack of scalable synthetic routes to produce graphene in the quantities required for industrial applications. The high cost of graphene production makes it inaccessible for commercial applications in several market segments including polymers, energy storage devices, and building materials such as concrete. The second problem relates to the low quality of graphene produced using most current commercial graphene manufacturing techniques. The most popular graphene production methods are based on graphite exfoliation through mechanical, chemical, or electrochemical treatments. However, a recent comparative study performed on different grades of graphene flakes provided by the top global graphene suppliers confirms that most of what is currently labeled and priced as graphene is actually graphite powder and none of these graphene manufacturers are capable of producing true graphene in a large-scale and cost-effective manner [9].

Previously, under agreement number DE-FE0031794 titled *Conversion of Domestic US Coal into Exceedingly High-Quality Graphene*, Rice University researchers studied the production of high value graphene from coal at gram scales using Flash Joule Heating (FJH) in a laboratory environment [10, 11]. Building upon these efforts and with aim to increase the technology readiness level (TRL) of the FJH based feedstocks, the primary objectives of cooperative agreement DE-FE0031988 (this project) were to optimize the FJH process for coal-based feedstocks and use statistical modeling (SM) techniques to improve outcomes of the FJH process. Additional objectives of the project included validating the technical and economic benefits of the production of graphene by FJH and development of applications in strategically chosen markets to maximize the cost and performance advantages as well as the environmental benefits that can be realized by the incorporation of coal derived graphene-based modifiers into different end-use applications.

## Development of Flash Joule Heating Systems

In order to initiate efforts aimed at addressing the objectives of this project, we first built the direct current (DC) mode to draw power from a bank of capacitors (96 capacitors with 1.1 F total capacitance) through pulse width modulation. For switching the high current, insulated-gate bipolar transistor (IGBTs) are used for switching up to 1000 Hz. While DC FJH with a capacitor bank is possible, it requires a complicated system as well as intensive labor. Therefore, we explored the possibility of using alternating current (AC) as an alternative for the DC system. Subsequently, using an available 480 VAC three phase system, we constructed an AC FJH system with 277 VAC and 100 A continuous capability (Figure 1). Although the system cannot provide thousands of amps, it is capable of providing hundreds of amps in longer period of time comparing to the DC system. Figure 2 and Figure 3 show the AC FJH system and its circuit diagram. Because the AC power line has a continuous current rating of 100 A, a current limiting capacitor was installed in series with the sample. This capacitor effectively limits the current to approximately 300 A. The system's switching is controlled by two silicon controlled rectifiers (SCRs) in parallel for full wave switching. This FJH system provides a longer flash duration with a peak current of 300 A. The two (2) second longer flash accumulates more energy than the DC flashing system. As the result, a 20 g sample of metallurgical coke (met coke) was successfully converted to graphene using this new FJH system. The AC peak current was measured to be up to 300 A with a clean sine wave profile) suggesting the clean Joule heating without sign of arc flash.

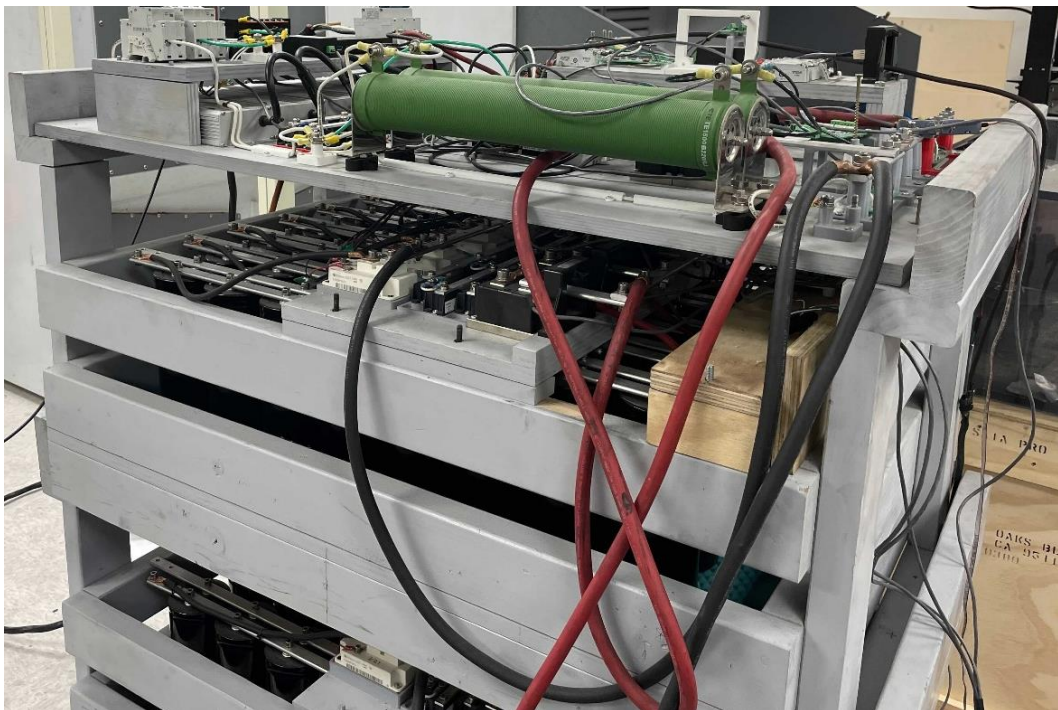


**Figure 1.** Flash Joule Heating system at Universal Matter's Houston Innovation Center

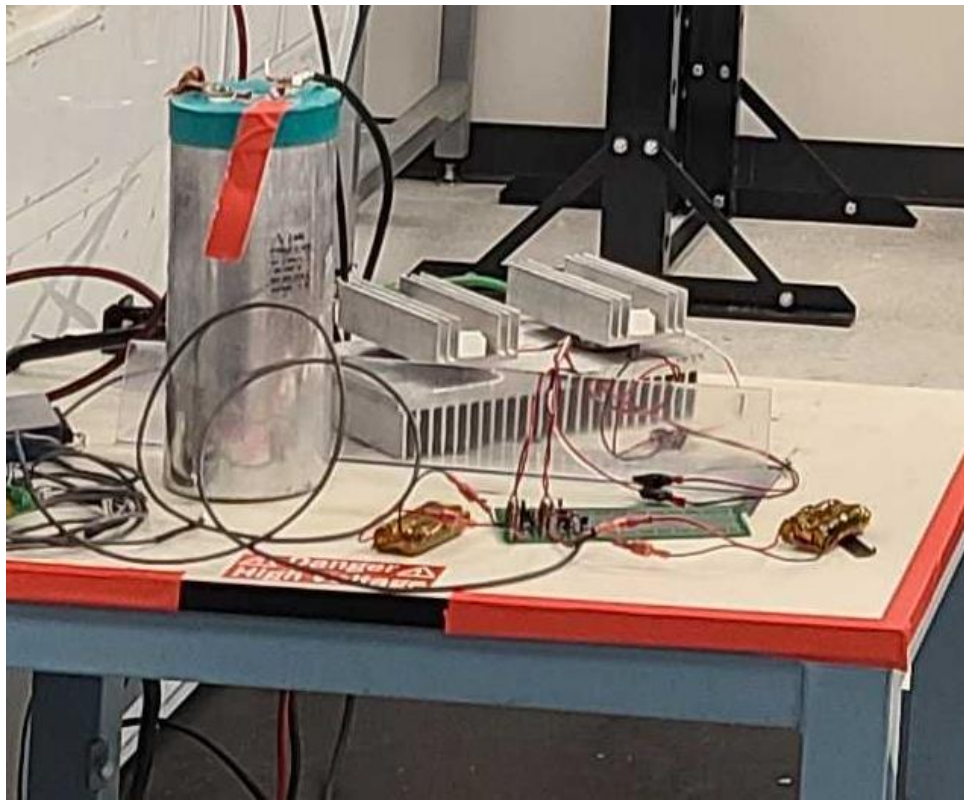


**Figure 2.** Prototype AC Flash Joule Heating system

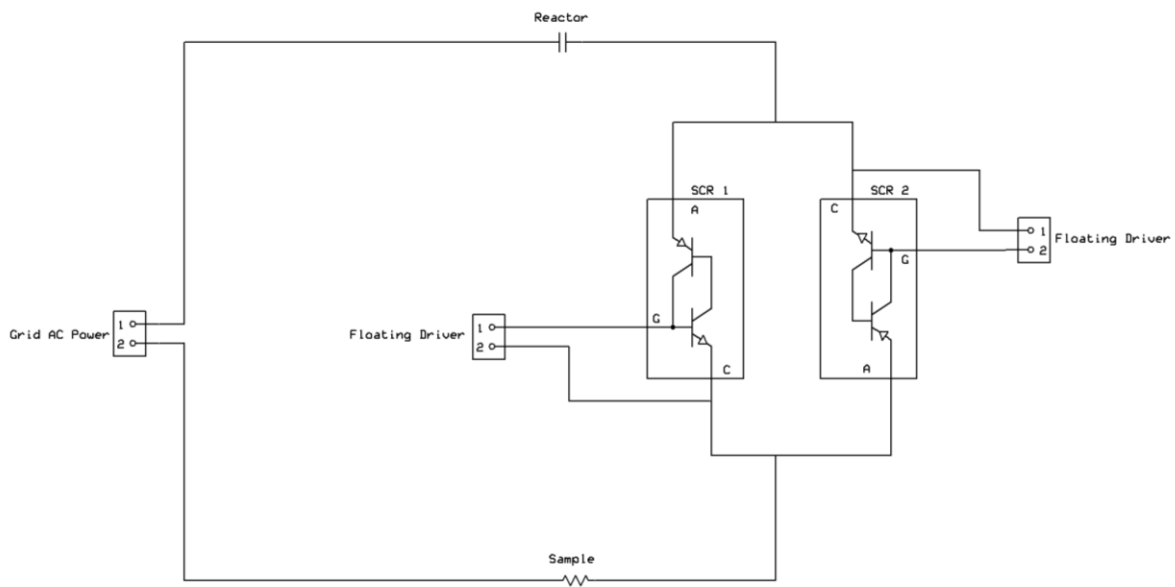


**Figure 3.** Circuit diagram of the high-power AC Flash Joule Heating system

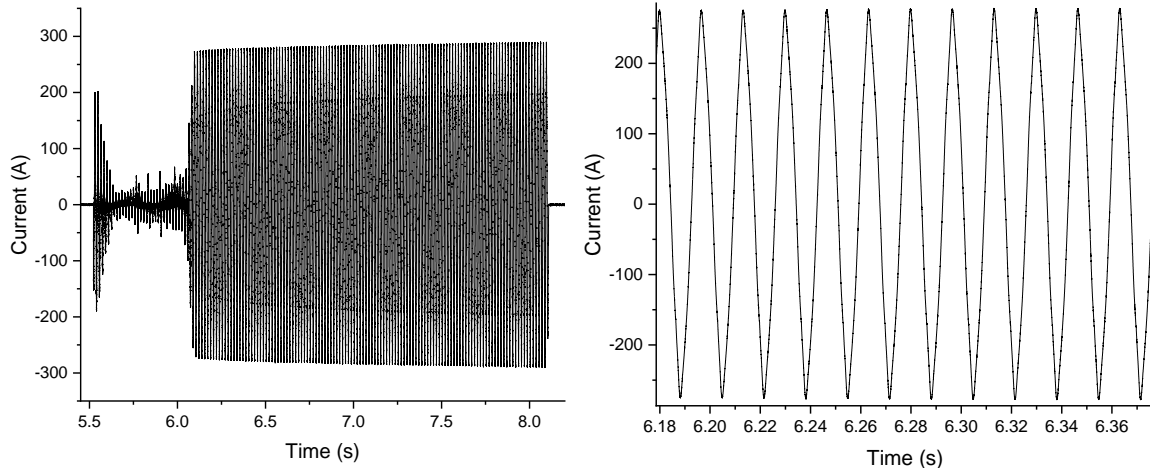
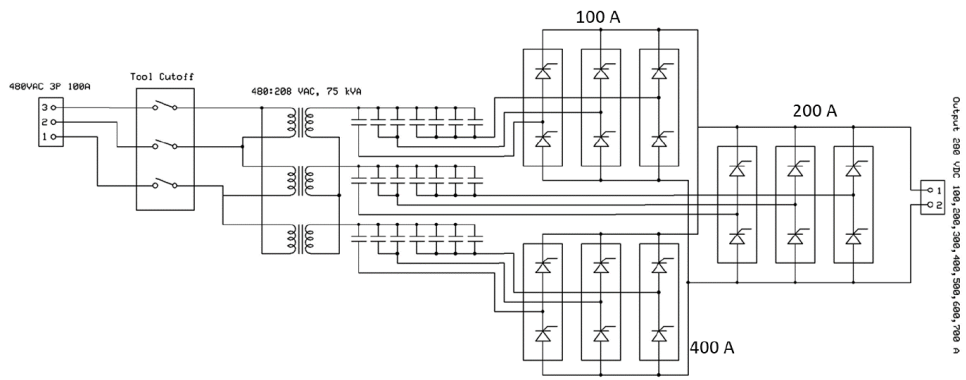


**Figure 4.** Electrical profile (current vs. time) of the Flash Joule Heating of 20 g of metallurgical coke

During experimentation with the AC FJH system, we observed that the voltage that was used for the FJH experiment lowered significantly towards the end of the flash. It was determined that the reason for this was due to a low resistance at the end of the flash, as the current reached the limiting current of the system. The power that was delivered to the sample was observed to be lowered as well. In order to have an efficient ACFJH system, the voltage and current must match the low resistance of the sample. The solution is to install a step-down transformer to lower the voltage from 480 VAC to 208 VAC and increase the current rating of the system from 100 A to 230 A. Accordingly, the flash switching system was also upgraded to accommodate the higher current rating.

The new current circuit is presented in Figure 6 and has an output is 280 VDC. Three parallel currents are regulated by a separated SCR switching system that allow for a current limit of 100 A, 200 A, and 400 A. Switching and combining the three switches allows for a current limit of 100 A to 700 A, with 100 A intervals. The controller also has a pulse width modulation mode that has a duty cycle of 5-100% on top of the current limiting control. Overall, the new FJH tool drives a much higher power with much better control of the system's power. Moreover, this system allows the operator to control the power input to the sample precisely, up to 150 kW.

With the newly built Flash Joule Heating (FJH) tool (Figure 5) in hand, we were able to successfully perform a FJH experiment on a 200 g sample of coal derived material (metallurgic coke or MC). Notably, the graphene product was found to have significantly improved properties, relative to past experiments. Furthermore, this achievement constituted a tenfold increase in the batch size amenable to FJH from the start of the project. Additionally, it is noted that the newly built FJH tool is substantially less costly (approximately one third of the cost) than the first DC flashing tool we had, while possessing the capability to perform FJH on a ten times larger sample batch size. Furthermore, all of the components of the new FJH tool are readily available from commercial vendors and lack apparent supply chain issues. These achievements demonstrate significant improvements in the cost efficiency of the FJH process that we have made in the first year of the project Importantly, in having successfully converted a 200 g batch of metallurgical coke to flash graphene (FG) using FJH, an objective of Subtask 5.1 was completed.



|                          |                       |
|--------------------------|-----------------------|
| Universal Matter Inc.    |                       |
| HIC Tool Power Schematic |                       |
| John J. Williams         | Rev 1.0<br>10/31/2022 |

**Figure 6.** Electrical schematic of the new Flash Joule Heating tool

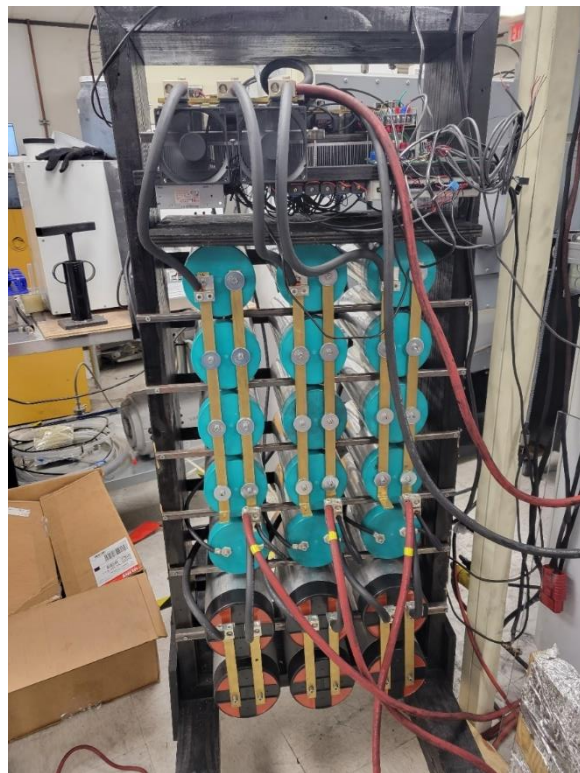


**Figure 5.** New Flash Joule Heating tool

## Further Development of Flash Joule Heating Systems

At first, the sample is flashed inside a homemade polycarbonate chamber (**Figure 7**). The sample holder jig is enclosed inside a polycarbonate chamber with exhaustion line. The jig provides compression to perform FJH on a sample of approximately 20 g which is enclosed in a 16 mm quartz tube. The jig is a linear stage that compresses the sample between two brass electrodes under two springs. The elasticity of the spring is needed to accommodate the dynamics of the FJH process, which results compression or expansion of the sample. A force sensor is integrated to the jig in order to record the pressure inside the sample.

Since the early stages of the development of the FJH process, we have been able to convert a large number of feedstocks into graphene [11]. However, in order to scale up and increase the current technology readiness level (TRL) of the FJH, a replacement for the flashing quartz tube to a more economically viable option was necessary. For example, for a 100 g FJH sample, the required quartz tube can cost upwards of \$50. When scaled up, the cost of the quartz tube is reduced, however, it can still be in range of \$200-300/kg of graphene produced. To reduce the cost of the FJH process, we experimented with different FJH reactor materials that included refractory cement, concrete, silicon carbide (SiC), ceramic, and refractory bricks. Gratifyingly, we found that refractory bricks, in the right configuration, are an excellent choice for an FJH reactor.

Figure 8 demonstrates the newly built FJH reactor comprised of refractory bricks. Instead of a one-piece cylindrical reactor, we found that rectangular configurations are also suitable for a FJH reactor. In the cylindrical reactor, the volatiles can only escape from the two side of the flashing tube. Therefore, we have seen many flashes that result in explosions because of the built up gas inside the reactor. With the rectangular brick reactor, the bricks have natural gaps between them. These gaps act as outgassing channels for the volatile products. As a result, we have not seen any explosion from the brick reactor. Furthermore, we have been able to safely scale up the FJH of up to 100 g of metallurgical coke using this reactor design. After performing FJH on the metallurgical coke inside the brick reactor, the top brick was removed, and the sample top surface temperature was measured to be 2200°C. This surface temperature is similar to the temperature during FJH of the same feedstock inside a quartz tube at 10 g scale reported from the first quarterly report. Using Raman spectroscopy, (Figure 9), we confirmed that the product obtained from FJH is in fact turbostratic graphene.



**Figure 7.** Flash Joule Heating chamber at Universal Matter's Houston Innovation Center

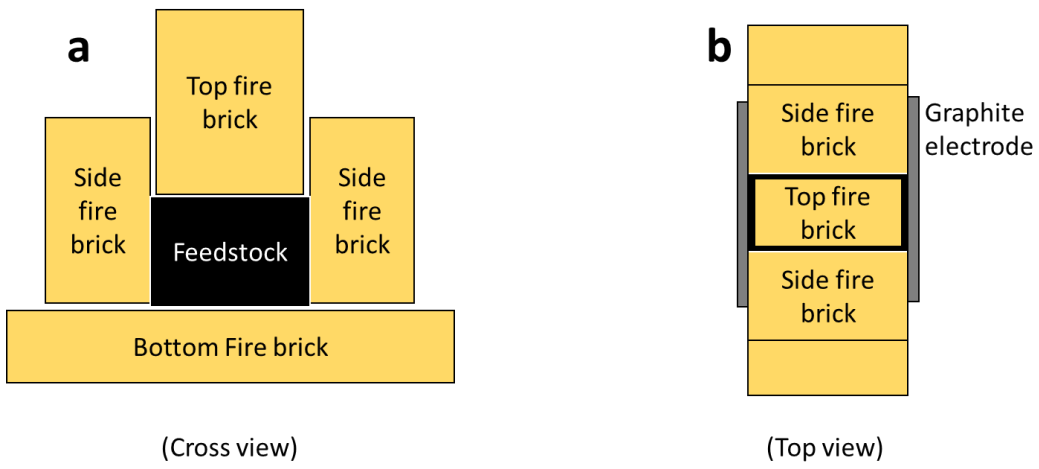


**Figure 8.** Layout of new Flash Joule Heating reactor constructed of refractory bricks

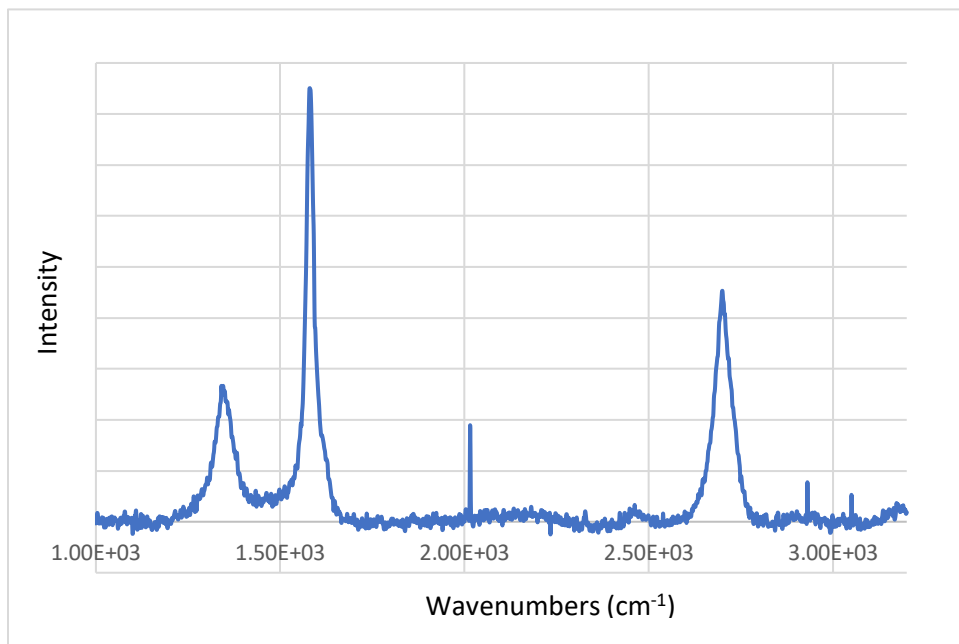


**Figure 9.** Raman spectrum of graphene obtained from Flash Joule Heating of metallurgical coke in the refractory brick Flash Joule Heating reactor

#### Flash Joule Heating of Bituminous Coal

Bituminous coal is one of the cheapest carbon feedstock in the coal and coke family. However, the carbon content of bituminous coal is much lower than that other coal feedstocks, such as anthracite coal and metallurgical coke; hence, we expected to face difficulty in converting bituminous coal to graphene using the FJH process. Accordingly, in order to prepare bituminous coal for a FJH experiment, mined bituminous coals were generally crushed and sieved to the size of 0.84-1.68 mm (#20 - #12 sieve size). In order to increase the conductivity of the feedstock, which is necessary for successful FJH, we tried two different methods:

- 1.) Mixing the bituminous coal with 10% of carbon black by mass. Unfortunately, performing FJH on this mixture was not successful due to high amounts of volatiles interrupting the current pathway. Energy dose that is necessary for graphene conversion was not reached and Raman spectra of the sample showed no 2D peak of graphene.
- 2.) Calcining the bituminous coal at 800°C. During calcining, a bituminous coal sample was found to lose 25% of mass as volatiles fuming out, however, this also increased the conductivity of the sample to be able to flash. The FJH of calcined bituminous coal started similar to the FJH of metallurgical coke but instead of increasing the current to the flashing point, the flash repeatedly stopped itself. One explanation for this phenomena is that the ash content of the sample remains high in the calcined bituminous coal. Therefore, instead of forming a carbon conductive pathway, the nonvolatile ash reacted with the carbon and decreased the conductivity of the sample to at least ten fold.

Based on this series of experiments, it is concluded that bituminous coal is not suitable a suitable feedstock for conversion to graphene using the FJH process due to its high ash and volatiles content.

## Flash Joule Heating of Metallurgical Coke

Metallurgical coke (MC) is a coal derived material that is produced from the pyrolysis of bituminous coal (metallurgical coal) [12]. In this project, metallurgical coke (MC) provided by SunCoke Energy was subjected to DC FJH with different pulse width modulation profiles. The MC feedstock was found to have good conductivity; thus, it was able to be subjected to FJH without further pretreatment. In the case of the DC FJH of MC, with a full time opening circuit, pretreatment of the sample by low voltage flashing is needed to avoid violent outgassing, which can result in an explosion. In a typical experiment, the flash is commenced after a few pretreatments and the peak current was found to be  $>1500$  A. With a Pulse Width Modulation (PWM) flash, a pretreatment of the sample is not necessary, and the peak current was measured to be  $<1000$  A, which reduces the flashing time, the risk of explosion during the experiment, and equipment failure, all while simultaneously increasing the process energy efficiency and production throughput.

As shown in Figure 10 b (black trace), the temperature profile measured during FJH experiments shows that the DC flash achieved nearly a  $3000^{\circ}\text{C}$  peak temperature and had a  $<500$  ms duration (Figure 10 a black trace), which matches well with previously published results [11]. Alternatively, the PWM flash was found to only peak at a temperature of approximately  $1600^{\circ}\text{C}$  (Figure 10 b – red trace), but has a duration of approximately 2 s. However, when analyzing the graphene quality by Raman spectroscopy, the two products are similar spectroscopically. Therefore, the combined results indicate that the lower temperature PWM FJH process can be compensated by a longer FJH time. Additionally, it is noted that despite the DC flash appearing to have a shorter duration, the production throughput using DC FJH is much lower than the PWM FJH process because of the addition of pretreatment flashes required in the DC process. Finally, the Variable Frequency Drive (VFD) frequency is found to be optimized in the range of 100-10000 Hz with duty cycle range of 0-50%. The VFD flash employs a soft start, common for electric motor starting, when a low duty cycle is first engaged to slowly heat the sample to remove some of the volatiles.

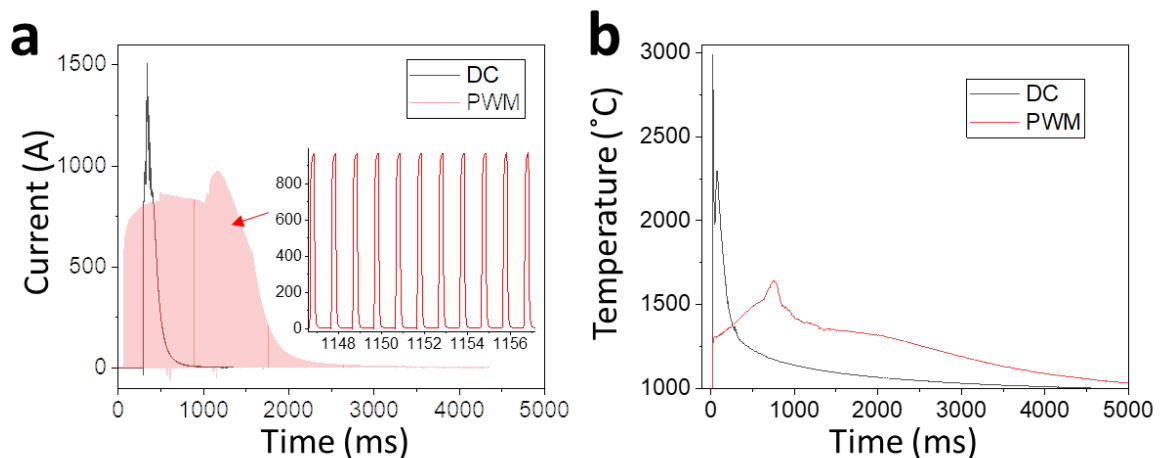


**Figure 10.** Current (a) and temperature (b) profiles vs. time of a DC flash (a) vs. a PWM flash (b). Note: The pulse sequence of the PWM flash is shown in the inset

X-ray diffraction (XRD) analysis of the product obtained from the FJH of MC indicates good graphene conversion as demonstrated by the expanded (002) peak located at approximately  $26^\circ 2\Theta$  (Figure 11 a) which indicates that the structure of the graphene product is not AB stacked graphene, which will have a peak at  $27^\circ 2\Theta$ . Raman spectroscopic analysis clearly shows the typical graphene spectra with a 2D peak located at approximately  $2700\text{ cm}^{-1}$  (Figure 11 b) [11]. With a D/G ratio of 0.8 and 2D/G ratio of 0.6, the metallurgic coke turbostratic graphene (MCTG) has a defective structure. A comparison of the Raman spectra of graphene obtained from DC FJH and AC FJH is presented in Figure 12. Raman spectra of MCTG synthesized from DC and AC Flash Joule Heating. Based on high resolution transmission electron microscopy (TEM), the MCTG has a sheet structure with flake size of approximately  $1\text{ }\mu\text{m}$  (Figure 13). The TEM also demonstrates a few layers of misaligned graphene structure.

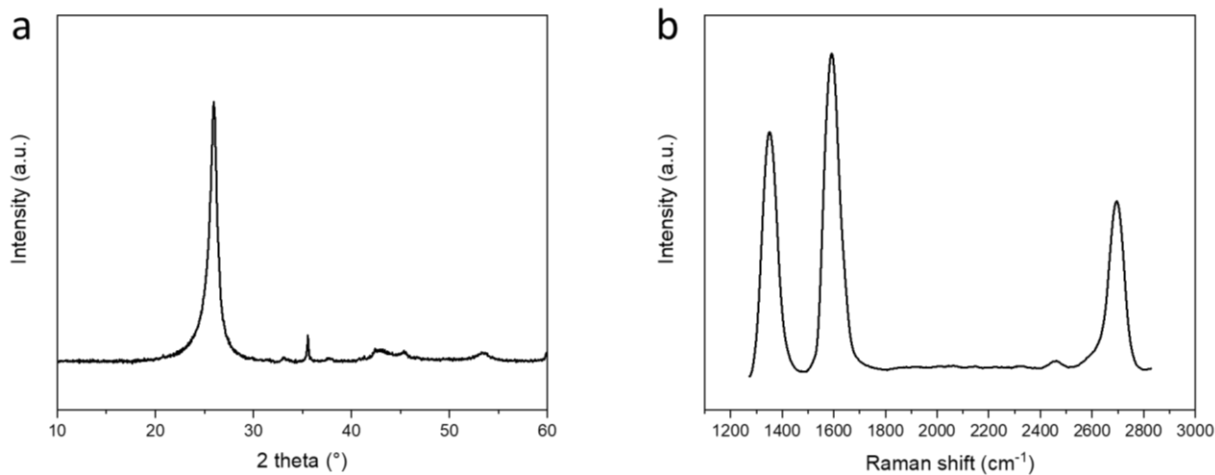


**Figure 11.** XRD (a) and Raman spectra (b) of turbostratic graphene synthesized from the Flash Joule Heating of metallurgical coke

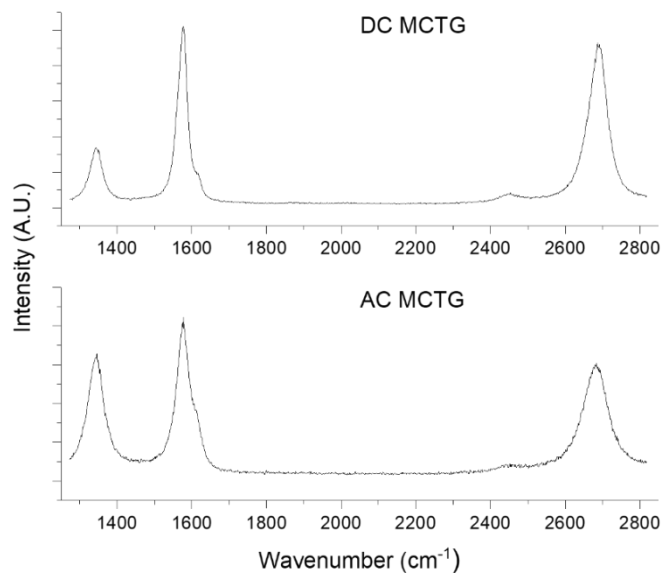


**Figure 12.** Raman spectra of MCTG synthesized from DC and AC Flash Joule Heating

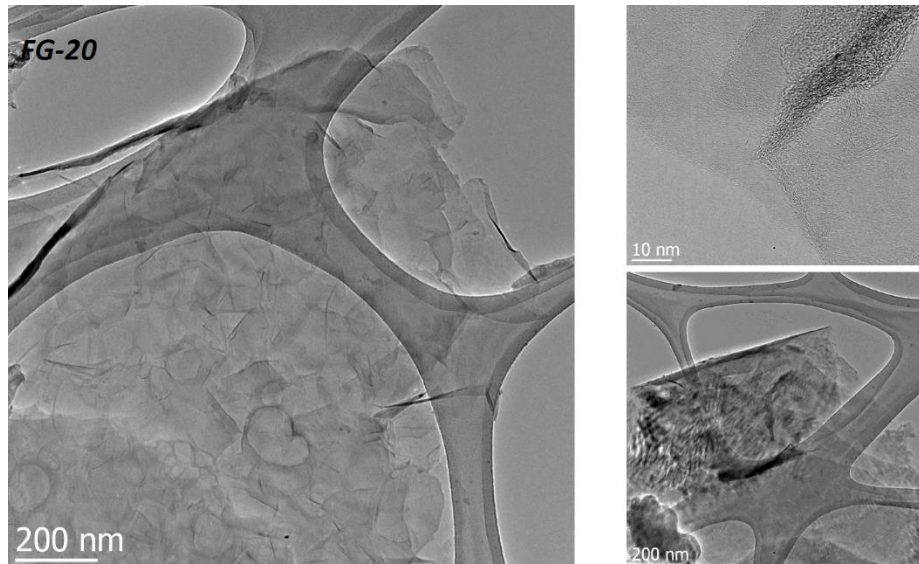


**Figure 13.** TEM characterization of metallurgical coke derived TG

#### Flash Joule Heating of Anthracite Coal

Anthracite coal has the highest carbon content amongst all coals and is envisioned as an inexpensive and abundant feedstock for product of graphene by FJH. According to the US Energy Information Administration (US EIA), in 2021 the average annual sale price of anthracite coal was approximately \$107 per short ton [13], which is significantly less than metallurgical coke, reported to be nearly \$400 per short ton.

In order to prepare samples of anthracite coal feedstock for FJH experiments, the coal was first crushed and sieved to #12-20 size. Subsequently, the resistance of a 5 g anthracite sample before FJH was found to be in the high range of  $k\Omega$  and enabled the direct FJH at approximately  $2\ k\Omega$ . Therefore, it was determined that anthracite should be treated with low dose AC flashing to initiate the conductivity. This pretreatment heat up the anthracite coal to reduce some of the volatile and increase the conductivity without flashing it. After treatment with AC, the anthracite coal sample was found to have resistance measured down to approximately  $150\ \Omega$ , and was deemed suitable for conversion to graphene by FJH. In a representative experiment, a 5 g anthracite sample was flashed with DC at 370 V, which successfully converted the starting material into turbostratic graphene (TG) with 70% yield. Raman spectroscopy shows single Lorentzian graphene 2D peak at  $\sim 2700\ cm^{-1}$  with low defect D peak at  $\sim 1350\ cm^{-1}$  (Figure 14).

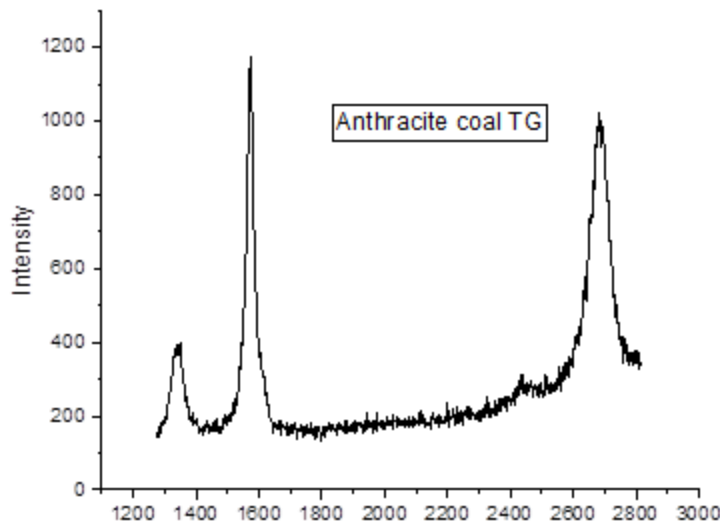


**Figure 14.** Raman spectrum of anthracite coal derived TG

In a quarterly report for this award (October, 2021), it was communicated that anthracite coal sourced from Pennsylvania was subjected to FJH after a high-temperature pretreatment, the purpose of which was to introduce conductivity to the material. In this experiment, it was found that the conversion of the anthracite coal to graphene was  $\sim 70\%$  and pretreatment was needed. Subsequently, anthracite coal was revisited as a FJH feedstock using a sample that was obtained from a separate source (Fisher Scientific - Victor, New York). The material sourced from Fisher was found to have a higher conductivity than the previously tested anthracite coal. As indicated by the Raman spectrum below (Figure 16), the higher carbon content anthracite coal demonstrated better conversion to graphene than the previously tested anthracite. This is evidenced by the low intensity D peak located at approximately  $1350\text{ cm}^{-1}$ , which indicates a low defect graphene structure [11]. Powder X-ray diffraction (XRD) was used as a secondary means to characterize the graphene synthesized from the FJH of anthracite coal, as well as the anthracite coal starting material itself. The X-ray diffractogram (Figure 15) demonstrates the evolution of the anthracite coal starting material from an amorphous carbon (with some impurities) to a material comprised of a high  $\text{sp}^2$  content, crystalline graphenic structure. As indicated by the green trace, the graphene obtained from the FJH process has the “cleanest” diffractogram, with a well-defined (002) peak at approximately  $27^\circ 2\Theta$  [11]. Furthermore, scanning electron microscopy (SEM) was also utilized to analyze the graphene product obtained from the FJH of anthracite coal. The SEM image in Figure 17 was obtained from a representative sample of anthracite derived graphene and demonstrates that the graphene flakes are  $1\text{-}2\text{ }\mu\text{m}$  in size, similar size to the Metallurgy coke derived FG and the CPC derived FG [11], with a relatively thin structure.

In summary, the work reported here has demonstrated that even amongst the same type of coal (anthracite), the unique feedstock identity plays a significant role in the process of FJH of coal to graphene. In fact, these investigations indicate that anthracite coals can have good conversion to graphene by FJH and yield graphene of suitable morphology, as confirmed by Raman spectroscopy, XRD, and SEM. Importantly, these results suggest that high carbon content anthracite coals may serve as an alternative to metallurgical coke as a coal-based feedstock for the production of graphene by FJH.

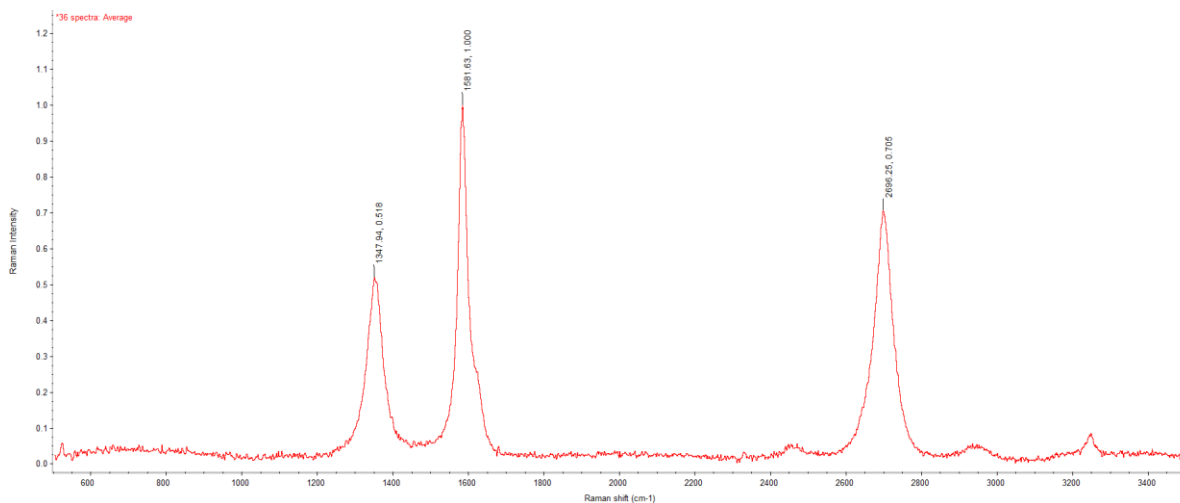


**Figure 16.** Raman spectra of anthracite coal derived flash graphene.

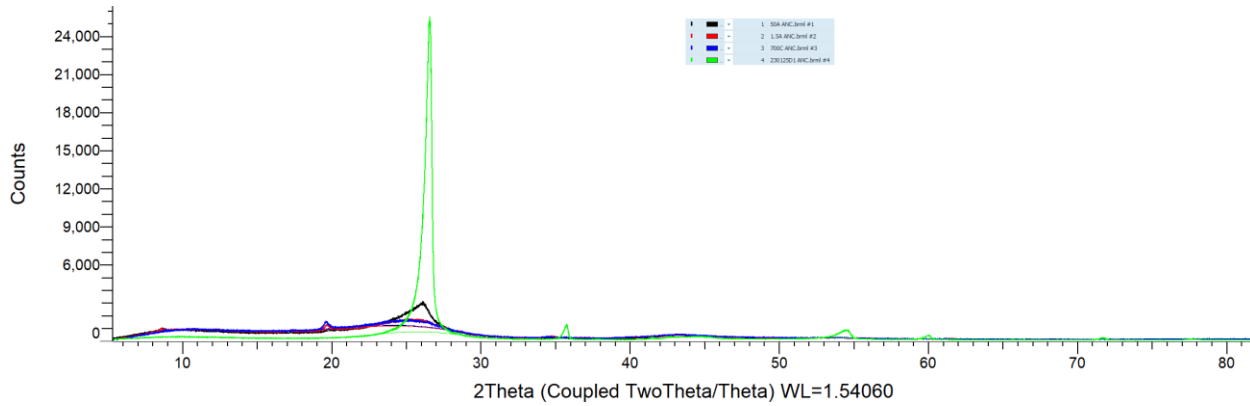


**Figure 15.** Overlayed X-ray diffractograms of anthracite coal and anthracite coal derived FG

Note: The blue and red in traces (diffractograms) correspond to the starting material/feedstock (anthracite coal sourced from NY) while the green trace is the graphene produced from the FJH of anthracite coal. The black trace corresponds to an “under-flashed” anthracite coal sample – indicating incomplete conversion to graphene.

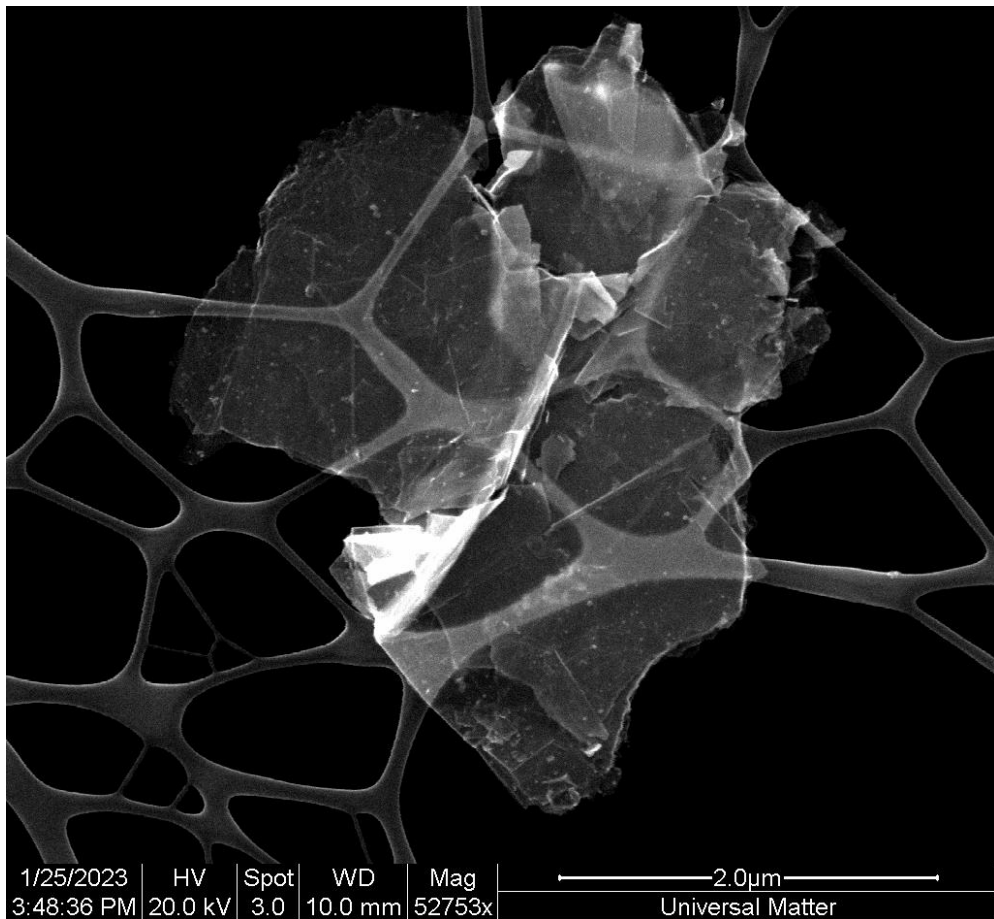


**Figure 17.** SEM image of an anthracite coal derived FG flake

#### Scale up of the Flash Joule Heating process: Achievements and challenges

In order to address further scale up of the FJH process, a collaboration was initiated with a high current testing laboratory to perform FJH on two samples (batches) of coal derived feedstock (metallurgical coke) on the order of approximately one (1) kilogram. In order to conduct FJH experiments for samples of this size, the collaborator provided a 2 MW power supply for the experiments. The size of the tube (sample container) that was used for the experiments was 75 cm in diameter. The testing results obtained from the two experiments are presented in Table 1. One of the samples had a mass of 0.7 kg while the other had a mass of 1.2 kg. In both instances, the yields of graphene obtained from the FJH of each sample of metallurgical coke were greater than 90% (91.9 and 90.9%, respectively). For the second sample, the flashing profile obtained from the experiment is presented in Figure 19. The peak current was measured to be 8 kA with a peak power approaching 2 MW. Raman spectroscopic characterization of the product obtained from the FJH of the 1.2 kg batch of metallurgical coke (Figure 19) shows the turbostratic structure of the graphene product with a single Lorentzian 2D peak at approximately  $2700\text{ cm}^{-1}$ . The low D/G ratio peaking at  $\sim 1350\text{ cm}^{-1}$  indicates the low defect structure of the graphene [14]. Overall, both of the samples passed our Raman quality control for graphene product, similar to our FG benchmark from smaller tube.

**Table 1.** Flash Joule Heating parameters obtained for metallurgical coke samples

| Size   | Mass (kg) | Duration (s) | Energy (MJ/kg) | $I_{2D/G}$  | $I_{D/G}$   | Yield       |
|--------|-----------|--------------|----------------|-------------|-------------|-------------|
| #12-20 | 0.7       | 5.413        | 6.57           | 0.557072594 | 0.314266592 | 0.919142857 |
| #12-20 | 1.2       | 11.46        | 6.11           | 0.536968925 | 0.383333931 | 0.909416667 |

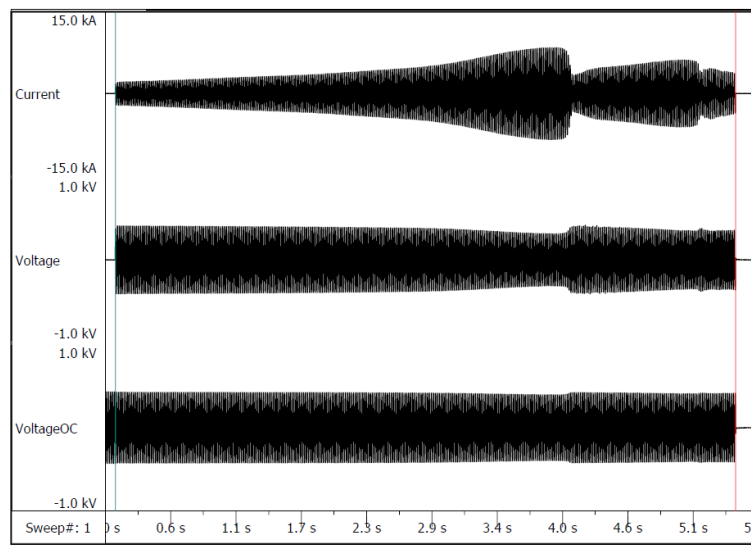


**Figure 19.** Profile obtained from the Flash Joule Heating of 1.2 kg of MC

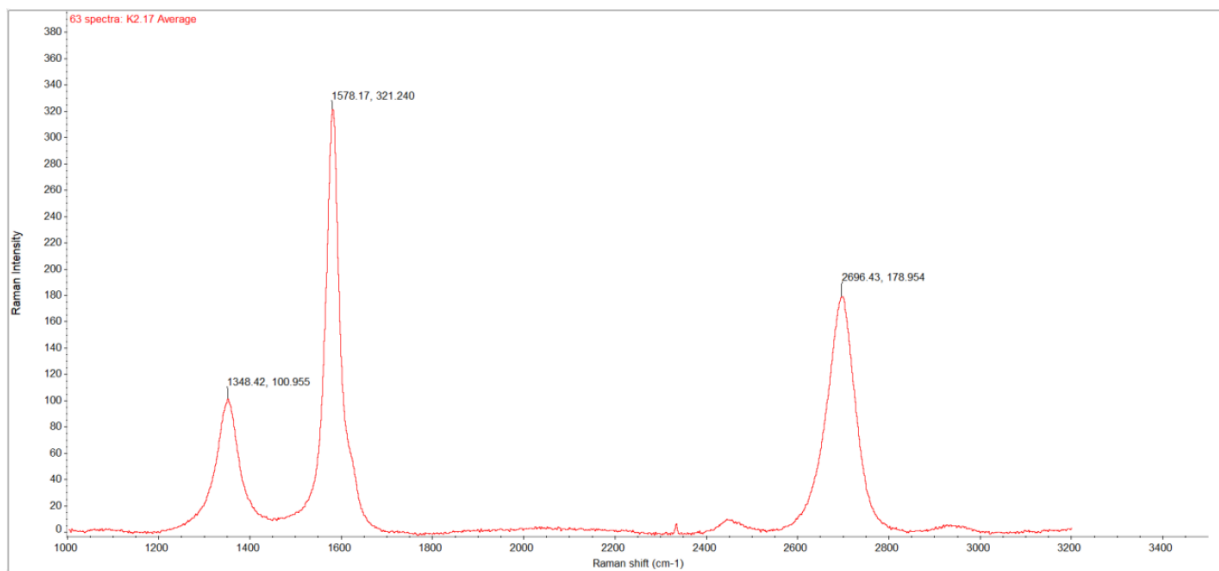


**Figure 19.** Raman spectrum of the product obtained from the Flash Joule Heating of 1.2 kg of MC

In order to further develop even larger scale FJH systems, carbon black (which can be coal derived) was chosen as an initial substrate, as it requires less power to flash than metallurgic coke. Thus, kilogram scale batches of carbon black can be flashed at once, making carbon black a suitable choice for proof of concept testing of a new larger scale Flash Joule Heating (FJH) reactor (jig). In addition, the carbon black induces less heat stress to the jig material and retains heat better than metallurgical coke. Accordingly, a 20 kg batch of carbon black was loaded a large trough constructed of refractory bricks (Figure 20, left and middle), which constitutes the larger scale FJH reactor. Note that the FJH assembly is made to compress the sample down by gravity. The top of the assembly is comprised of refractory material, while the middle is made from quartz, and the two ends are composed of graphite electrodes. In the experiment, the whole trough of carbon black was flashed section by section in order to convert all of the substrate into flash graphene product. After 4 hours of total FJH time, 15 kg of high and consistent quality graphene was produced in high graphene yield (>90% based on Raman) was collected (Figure 20, right). Raman, XRD and TEM confirmed graphene that is similar to the carbon black derived graphene from the original Nature paper [11].

We attempted to leverage a semi-automated FJH concept in order to transform a coal derived feedstock, metallurgical coke, to graphene. However, in doing so, we faced a critical problem. As demonstrated in Figure 22, the FJH reactor constructed of refractory bricks could not withstand the extreme heat associated with the FJH of metallurgical coke. The high temperature from the FJH process melted the refractory material and contaminated the graphene product. In order to mitigate the damage from the FJH process, it was decided that a new material for the FJH jig should be the next focus of research. First, we experimented with the use of a sacrificial layer, which included molding fine sand with an oil binder as the sacrificial layer. Initial results show that the sacrificial layer successfully protected the refractory brick during the FJH process, as demonstrated in Figure 22.



**Figure 20.** Semi-automated Flash Joule Heating reactor with carbon black substrate (left and middle) and graphene product (right)



**Figure 22.** Damage to Flash Joule Heating reactor components resulting from high temperature of Flash Joule Heating experiment



**Figure 22.** Sacrificial layer (molding sand) of Flash Joule Heating reactor after experiment

#### Development of a machine learning method for process optimization

Under this project, the foundations for our database (Figure 23-24) have been fully laid out and our team has implemented forms of automatic data-logging and analysis across most daily activities. Some aspects of the database and of the applications for interacting with said-database are still under development as we go through the learning process. By simply filling out sample details (either manually or imported), a sample can be tracked from cradle-to-grave, i.e., from its feedstock to its flashing (FJH), flashing to characterization, characterization to dispersion, and dispersion to testing. With these procedures being implemented team-wide, we are now able to draw connections from beginning to end on effects that produce quality graphene and resultant graphene products. The Python programs make data input and analysis into SQL backends quick and simple. Although not shown, we've utilized the Google Charts Application Programming Interface (API) to instantly create QR codes for rapid sample connection as well, which has increased the ease of tracking while also minimizing errors. Due to process improvements over the course of developing of the database, a large amount of previously collected data was determined to no longer meet our qualifications for tracking. However, as our production technology has stabilized, we expect to be able to build large datasets very quickly across many different feedstocks and applications.

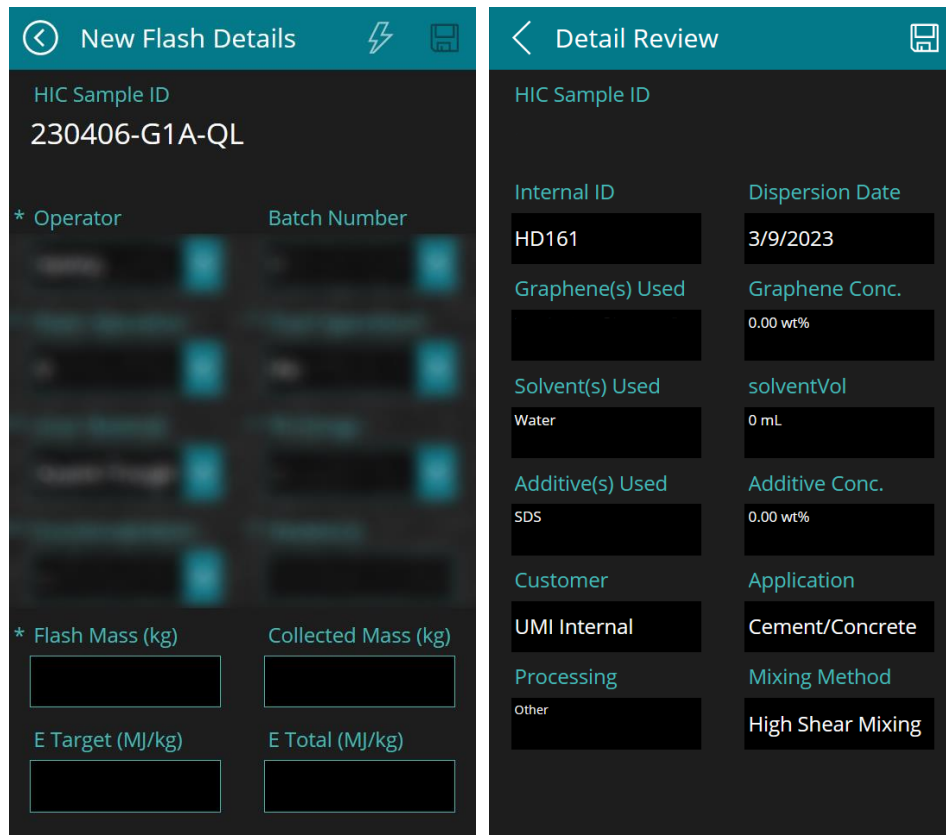


**Figure 23.** Screenshots from current database tracking app for Flash Joule Heating data and dispersion data

### Statistical modeling

Through the work of researchers at the University of Missouri, Columbia, (project team member) strong correlations between the electrical parameters of FJH and the resultant graphene product were elucidated. Initially, 42 large-scale tube flashes of metallurgical coke were investigated, with sample sizes ranging from 0.7 kg to 10 kg. Pre-processing of the data, shown below in Figure 24, was utilized to clean and scale the dataset for appropriate manipulation later. Without cleaning the data, parameters that are text or missing can prevent proper handling, and without scaling, features that are on completely different magnitudes, such as voltage and resistance, might be over- or under-represented. Analysis of the data was performed using Python packages for generating distribution plots to visualize flash parameters as continuous probability density curves with kernel density estimates (KDE), as shown below in Figure 25. Violin plots, which are similar to box plots with the aforementioned kernel density estimates, were also generated, and are shown in Figure 26.

| No | F1        | F2    | F3  | F4 | F5  | F6   | F7  | F8   | F9   | F10  | F11  | F12 | F13 | F14  | F15  | F16  | F17  | F18  | F19  | F20  | F21  | F22  | F23  | F24   | R    |
|----|-----------|-------|-----|----|-----|------|-----|------|------|------|------|-----|-----|------|------|------|------|------|------|------|------|------|------|-------|------|
| 1  | 10        | 100   | 1   | 1  | 0   | 1    | 54  | 7.5  | 37.1 | 16.1 | 0.59 | 16  | 480 | 3.06 | 2.26 | 5.07 | 1.08 | 3.22 | 0.58 | 0.08 | 6.89 | 3.03 | 15.6 | 376   | 0.94 |
| 2  | 10        | 100   | 1   | 1  | 0   | 1    | 54  | 7.5  | 34.5 | 16.1 | 0.47 | 11  | 300 | 15   | 2.05 | 7.13 | 0.62 | 2.47 | 0.43 | 0.26 | 1.64 | 6.96 | 63.3 | 233.5 | 0.47 |
| 3  | 10        | 100   | 1   | 0  | 1   | 1    | 54  | 7.5  | 35.6 | 16.1 | 0.9  | 11  | 300 | 9.9  | 2.34 | 8.09 | 0.7  | 2.68 | 0.01 | 0.04 | 0.24 | 5    | 54.2 | 207   | 0.5  |
| 4  | 10        | 100   | 0.4 | 1  | 0   | 1    | 42  | 7.5  | 25.7 | 16.1 | 0.46 | 11  | 300 | 10   | 1.09 | 2.38 | 0.33 | 1    | 0.43 | 0.23 | 1.87 | 2.97 | 11.8 | 194   | 0.28 |
| 5  | 10        | 100   | 0.4 | 0  | 1   | 1    | 42  | 7.5  | 25.4 | 16.1 | 0.36 | 11  | 300 | 7.54 | 1.4  | 2.9  | 0.42 | 1.19 | 0.71 | 2.32 | 0.31 | 2.86 | 1.47 | 164.4 | 0.21 |
| 6  | 10        | 100   | 1   | 0  | 1   | 0.7  | 42  | 7.5  | 25.1 | 16.1 | 0.31 | 11  | 300 | 5.41 | 3.45 | 8.46 | 1.03 | 2.68 | -0   | 0.23 | -0.1 | 4.6  | 64.3 | 253.4 | 0.31 |
| 7  | 10        | 100   | 1   | 1  | 0   | 1.2  | 54  | 7.5  | 33.3 | 16.1 | 0.41 | 11  | 300 | 11.5 | 2.55 | 7.14 | 0.77 | 2.5  | 0.04 | 0.22 | 0.16 | 7.33 | 74.5 | 235.5 | 0.38 |
| 8  | 10        | 100   | 1   | 0  | 1   | 1.4  | 54  | 7.5  | 33   | 16.1 | 1.49 | 11  | 300 | 19   | 1.74 | 6.5  | 0.52 | 2.36 | 0.98 | 0.09 | 10.7 | 7.16 | 57.7 | 296.2 | 0.47 |
| 9  | 10        | 0 1 0 | 0   | 1  | 0   | 1    | 54  | 7.5  | 35.5 | 16.1 | 0.76 | 16  | 480 | 2.68 | 2.83 | 8.94 | 1.36 | 5.21 | 0.6  | 0.08 | 7.45 | 3.04 | 21.4 | 384.7 | 0.93 |
| 10 | 10        | 100   | 1   | 0  | 1   | 1.96 | 74  | 7.5  | 51   | 16.1 | 0.74 | 11  | 300 | 19   | 2.22 | 5.88 | 0.66 | 2.2  | 0.42 | 0.08 | 5.29 | 10.7 | 93.3 | 273.1 | 0.36 |
| 11 | 10        | 0 0 1 | 1   | 1  | 0   | 1    | 54  | 7.5  | 34.2 | 16.1 | 0.82 | 16  | 480 | 3.29 | 2.1  | 5.12 | 1.01 | 3.29 | 0.68 | 0.16 | 4.29 | 3.02 | 14.5 | 340.4 | 0.78 |
| 12 | 10        | 100   | 1   | 1  | 0   | 1    | 54  | 7.5  | 36.1 | 16.1 | 0.6  | 16  | 480 | 5.65 | 2.52 | 6.97 | 1.21 | 3.81 | 0.56 | 21.9 | 0.03 | 5.98 | 35.8 | 382.8 | 0.37 |
| 13 | 10        | 0 0 1 | 1   | 1  | 0   | 1    | 54  | 7.5  | 34.9 | 16.1 | 0.95 | 16  | 480 | 5.39 | 2.89 | 9.53 | 1.39 | 4.45 | 0.82 | 0.18 | 4.66 | 6.09 | 44.9 | 324.3 | 0.77 |
| 14 | 10        | 100   | 0   | 1  | 0   | 1    | 54  | 7.5  | 34.5 | 16.1 | 0.43 | 16  | 480 | 3.35 | 4.42 | 9.79 | 2.12 | 5.56 | 0.57 | 0.12 | 4.83 | 6.03 | 65.5 | 415.6 | 0.4  |
| 15 | 10        | 100   | 1   | 1  | 0   | 1    | 54  | 7.5  | 35.5 | 16.1 | 0.45 | 11  | 300 | 9.83 | 2.54 | 7.45 | 0.76 | 2.56 | 0.59 | -0.1 | -5.3 | 5.97 | 63.2 | 199.9 | 0.43 |
| 16 | 10        | 100   | 1   | 1  | 1   | 1    | 54  | 7.5  | 38   | 8    | 0.68 | 4.4 | 300 | 7.61 | 1.38 | 3.26 | 0.41 | 0.98 | 0.48 | 0.12 | 3.92 | 3.14 | 0.23 | 14.4  | 0.87 |
| 17 | 10        | 100   | 1   | 1  | 1   | 5    | 84  | 12   | 82.1 | 8    | 0.76 | 2.6 | 300 | 119  | 1.33 | 3.01 | 0.4  | 0.9  | 0.5  | 0.18 | 2.73 | 32.5 | 0.18 | 210   | 0.48 |
| 18 | 10        | 100   | 1   | 1  | 1   | 1    | 54  | 7.5  | 36.9 | 8    | 0.62 | 4.4 | 300 | 18.3 | 1.2  | 3.31 | 0.36 | 0.99 | 0.49 | 0.47 | 1.04 | 6.49 | 0.27 | 26.4  | 0.59 |
| 19 | 10        | 100   | 1   | 1  | 1   | 1    | 54  | 7.5  | 31.6 | 8    | 0.65 | 4.4 | 300 | 15   | 1.18 | 2.65 | 0.35 | 0.79 | 0.47 | 0.28 | 1.68 | 5.25 | 0.27 | 20.7  | 0.67 |
| 20 | 10        | 100   | 1   | 1  | 1   | 1    | 54  | 7.5  | 36   | 8    | 0.56 | 2.6 | 300 | 22   | 1.77 | 3.23 | 0.53 | 0.97 | 0.46 | 0.04 | 12.1 | 5.89 | 0.11 | 69.5  | 0.49 |
| 21 | 10        | 100   | 1   | 1  | 1   | 1    | 54  | 7.5  | 34.8 | 8    | 0.67 | 2.6 | 300 | 31   | 1.83 | 3.26 | 0.55 | 0.98 | 0.45 | 0.03 | 16.1 | 7.61 | 0.11 | 104.8 | 0.35 |
| 22 | 10        | 100   | 1   | 1  | 1   | 2    | 84  | 7.5  | 73   | 8    | 1.07 | 2.2 | 600 | 22   | 1.54 | 2.88 | 0.92 | 1.73 | 0.77 | 0.28 | 2.75 | 12.1 | 0.26 | 53.7  | 0.45 |
| 23 | 10        | 100   | 1   | 1  | 1   | 4.5  | 54  | 12   | 81   | 8    | 0.96 | 2.6 | 600 | 65.5 | 1.39 | 1.07 | 0.84 | 0.64 | 0.39 | 1.62 | 0.24 | 28.2 | 0.32 | 127   | 0.5  |
| 24 | 10        | 100   | 1   | 1  | 1   | 10   | 102 | 15   | 82.5 | 8    | 1    | 2.2 | 600 | 82   | 1.23 | 2.76 | 0.74 | 1.65 | 0.86 | 0.12 | 7.08 | 27.2 | 0.39 | 125   | 0.75 |
| 25 | 0 1 0 0 1 | 1     | 1   | 1  | 1.5 | 42   | 7.5 | 28.3 | 8    | 3.3  | 2.6  | 300 | 30  | 1.44 | 3.22 | 0.43 | 0.97 | 2.01 | -0   | -279 | 6.93 | 0.17 | 61.1 | 0.4   |      |

**Figure 24.** Screenshot of Flash Joule Heating datasets after data cleaning and handling categorical features.

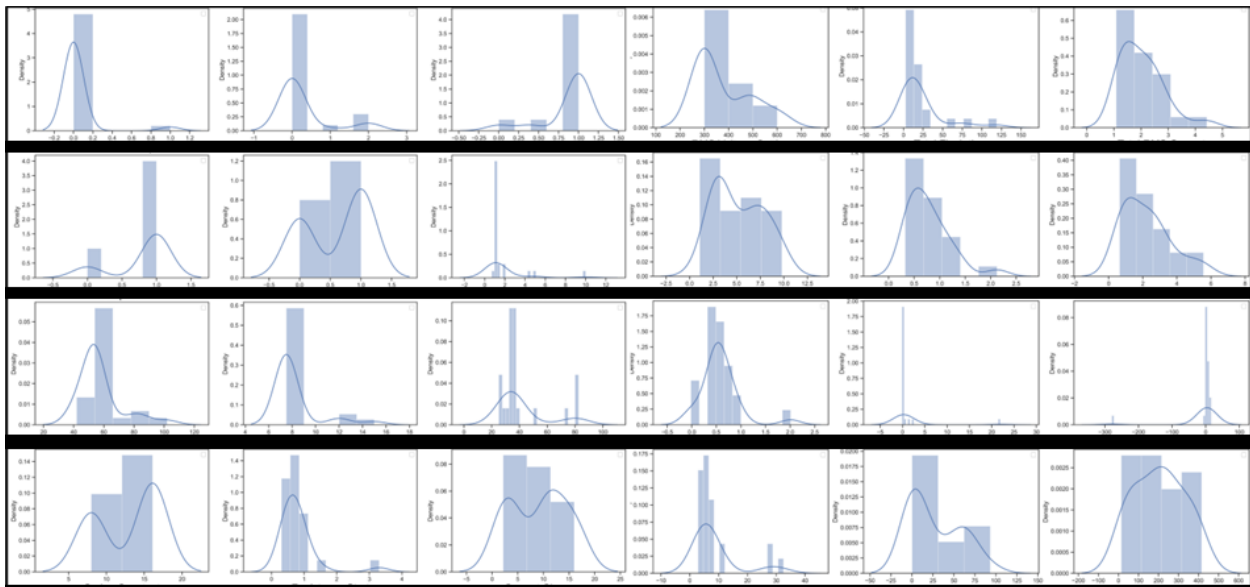


**Figure 25.** Distribution and kernel density estimates plots of the whole dataset

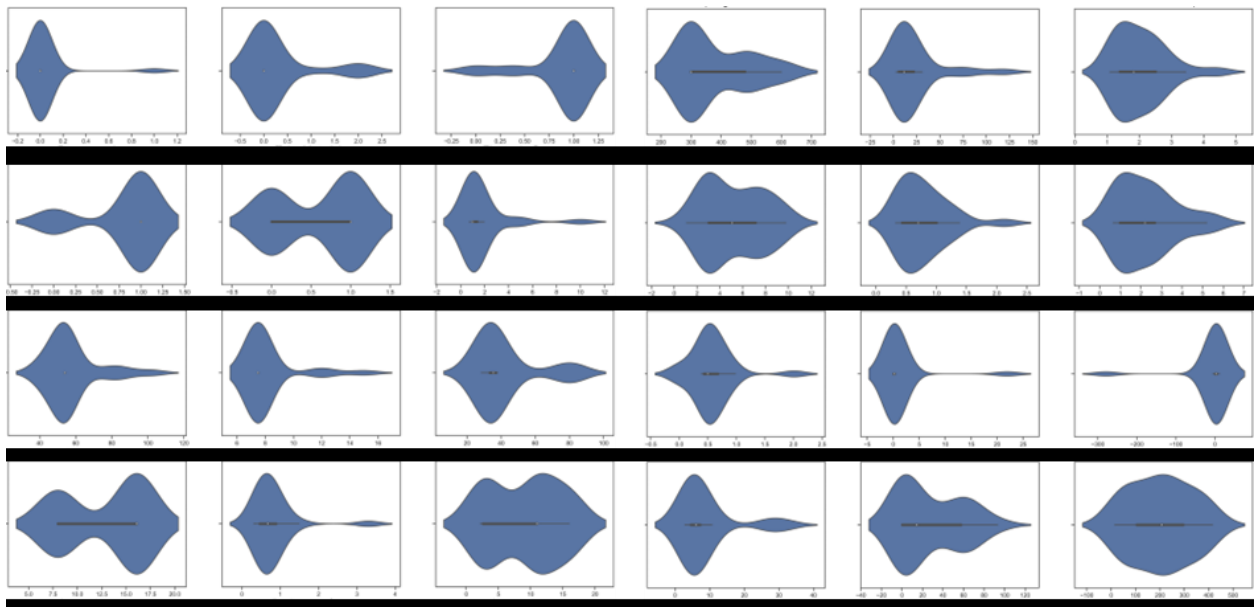


**Figure 26.** Violin plots of the dataset

Through calculating Pearson correlation coefficients, linear relationships between parameters were drawn. The parameters range from -1 to 1, where -1 is a complete negative correlation, 0 means no correlation at all, and 1 is a complete positive correlation. Figure 27 illustrates a heatmap drawn from the Pearson correlation coefficients. Features that showed an almost perfect correlation are removed from model training to improve model accuracy.

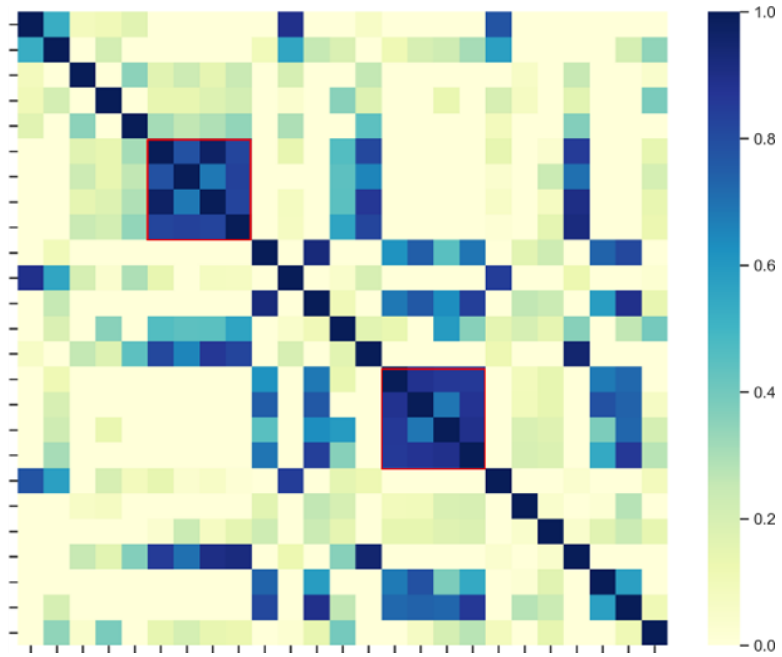


**Figure 27.** Pearson correlation coefficient matrix of the Flash Joule Heating parameters

While the analysis represents a significant suite of strong statistical, there are still many steps left in ensuring that the eventual model is representative. For example, these next steps include transforming data from small-scale metallurgical coke FJH runs to connect the laboratory-scale and pilot-scale data, as well as inputting data from similar small-scale FJH runs from high-purity feedstocks, in order to isolate effects of feedstock composition on flash performance and quality.

#### Evaluation of graphene in different applications

Development of method to disperse metallurgical coke turbostratic graphene

We found that metallurgical coke derived FG (MC-FG) is not able to be readily exfoliated in either aqueous or organic solvents. Figure 28 shows an SEM image of MC-FG after ball milling for size reduction of the #12-20 mesh size grain. Therefore, the dispersion of MC-FG in solution is an order of magnitude smaller than the FG made with carbon black as the feedstock. Accordingly, under this project, we sought to find an effective post-processing method to exfoliate the MC-FG. Various methods have been tested and include:

- 1.) Mechanical exfoliation through high shear mixing and media milling
- 2.) Chemical milling exfoliation
- 3.) Hydrothermal intercalation with iron and exfoliation
- 4.) Electrochemical exfoliation

Of all methods list above, we found that only chemical milling effectively exfoliated the MC-FG. As shown in Figure 29, the chemical milling post-process treatment increases the dispersion of MC-FG at least three times as compared to the untreated MC-FG. SEM and TEM micrographs presented in Figure 30 and Figure 31 show that after chemical milling the MC-FG has been successfully exfoliated into graphene of a few-layers and with flake sizes of approximately 500 nm. The experimental process for exfoliation by chemical milling is as follows:

- 1.) A 100 g batch of metallurgical coke (provided by SunCoke Energy) is sieved to #12-20 mesh and subjected to FJH to produce MC-FG
- 2.) MC-FG (1.8 g), pyrene or hydroquinone (Figure 31) 9 g (Pyrene/MC-FG = 5), Yttria-stabilized zirconia (YSZ) 10 mm balls 56 g (ball to powder ratio = 93) are put into a ball mill and milled at 700 rpm for 100 minutes. After milling, the balls and powder are sieved through a #20 mesh. The milled mixture is then added to 250 ml of acetone to dissolve the pyrene (or hydroquinone). The FG is then filtered and washed with acetone.
- 3.) To test the dispersibility, 0.05% of MC-FG is dispersed in N-Methyl pyrrolidone (NMP) using a high shear mixer at 9000 rpm for 5 minutes, then centrifuged for 5 minutes at 500 RCF (Relative centrifugal force). A UV-vis spectrum is measured to determine the absorption of the dispersion before and after centrifugation.

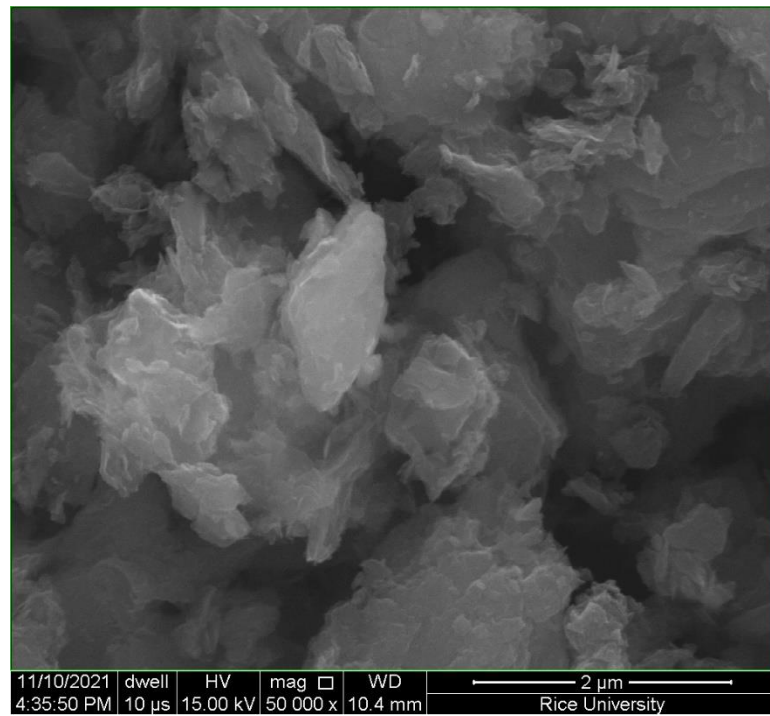


**Figure 28.** SEM image of Flash Graphene derived from metallurgical coke

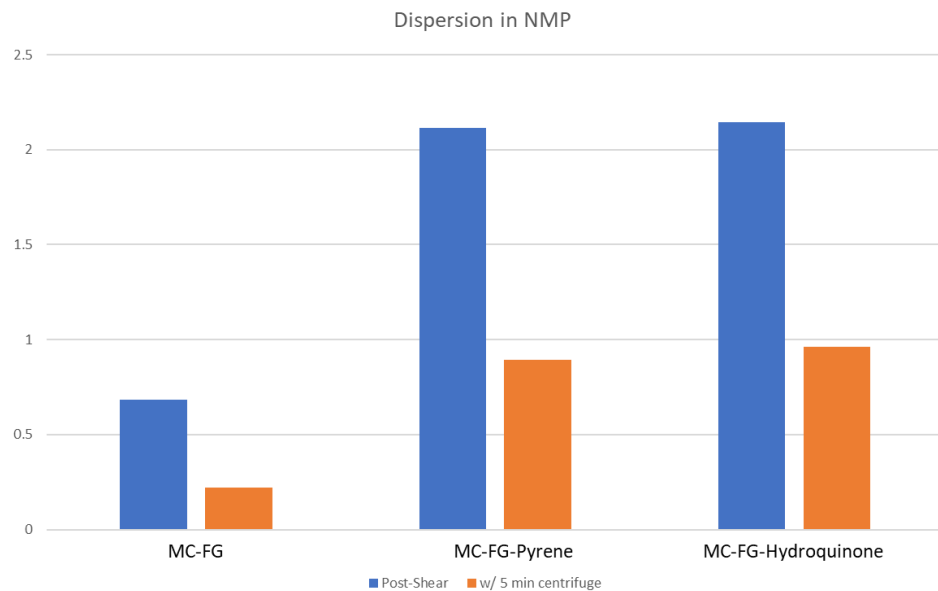


**Figure 29.** UV-vis absorption for various dispersions (in NMP) of untreated MC-FG, MC-FG after the pyrene milling process ("MC-FG-Pyrene"), and MC-FG after the hydroquinone milling process ("MC-FG-Hydroquinone")

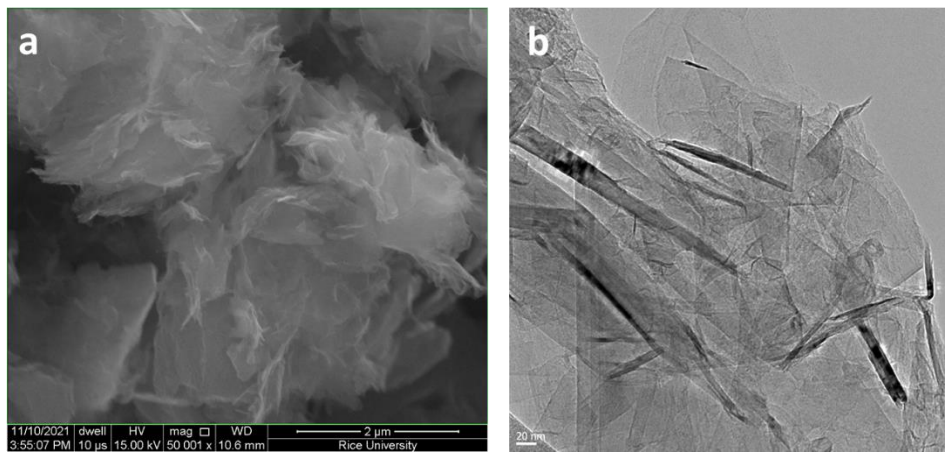


**Figure 30.** SEM and TEM images of MC-FG after the pyrene milling process

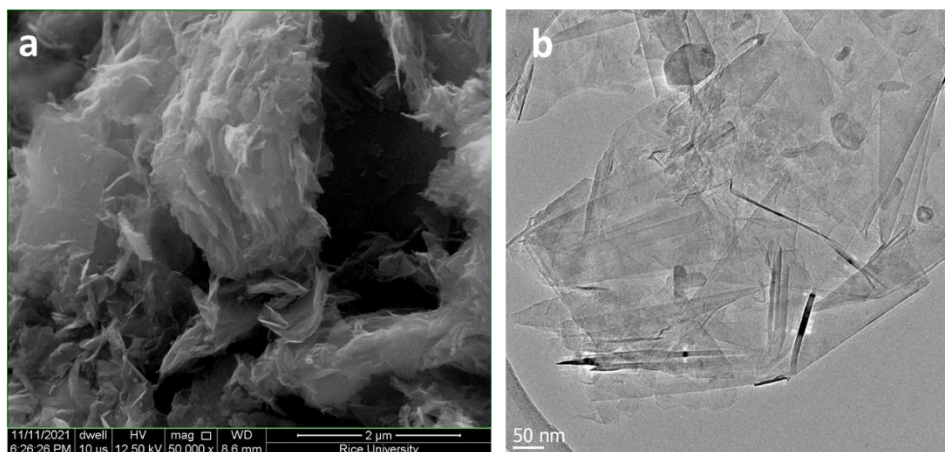


**Figure 31.** SEM and TEM images of MC-FG after the hydroquinone milling process.

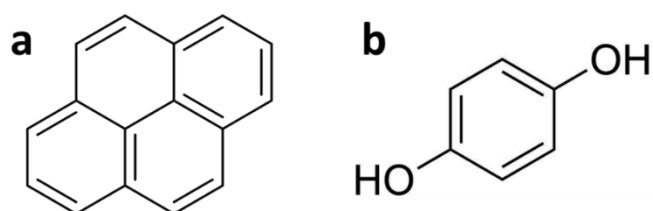


**Figure 32.** Chemical structures of pyrene (a) and hydroquinone (b)

Flash graphene in concrete

Samples of MC-TG, were tested to assess performance of the material in the reinforcement of concrete. General use limestone (GUL) cement, potable water, MC-FG, sand and limestone with 19 mm in size were used to prepare concrete cylindrical specimens with dimensions of 4" by 8". The mix-design chosen for making the 1 m<sup>3</sup> concrete specimens was 250 kg/m<sup>3</sup> cement, 864 kg/m<sup>3</sup> sand, 1130 kg/m<sup>3</sup>

stone, 167.5 kg/m<sup>3</sup> water, 250 ml admixture per 100 kg cementitious content. The MC-FG dispersion at the required concentration (% by weight of cement) was prepared in water using a high speed shear-mixer (Silverson L5M Model) at 5000 rpm for 15-20 minutes. The as-prepared MC-FG dispersion was then mixed with the rest of the ingredients in a drum-type mixer during the batching. Standard practices outlined both in Concrete Standard Practices CSA A23.1:19/A23.2:19 and ASTM C192 were followed for making and curing the concrete specimens. During the batching, it was ensured that the moisture for sand and stone were corrected and any free-moisture (if present) was subtracted from the total amount of batching water. The concrete thus was poured in three equal layers into plastic molds and each layer was consolidated using 20 strokes of a tamping rod. The molds were sealed from the top using lids and the cylindrical specimens were demolded after 24 hours and transferred to lime-saturated water for curing. The specimens that were cured for 7-days were tested for their compressive strength using a Forney Automatic Compression Testing Machine (Figure 33). Steel caps with neoprene pad cushioning were used for capping the concrete cylinders as outlined in ASTM C 1231. The rate of loading during compressive strength testing was within the range of 0.15 MPa/s to 0.35 MPa/s as outlined in ASTM C 39. The average compressive strength of three specimens was taken as the representative compressive strength. The results showed an improvement of approximately 9% in compressive strength of cement with MC-FG as compared to a reference sample, which is a promising result as only 0.1% MC-FG by mass was added to the concrete (Table 2).



Figure 33. Photographs of concrete sample production (left), concrete samples (middle left), and sample testing (middle right, right)

**Table 2.** Compressive strength results from concrete control samples and MC TG reinforced concrete samples

|                | Control      | 0.1% UM0701XP Concrete (Union Process) |
|----------------|--------------|--|
|                | 20.99        | 22.82                                  |
|                | 21.33        | 23.61                                  |
|                | 21.79        | 23.67                                  |
|                | Control      | 0.1% UM0701XP Concrete (Union Process) |
| <b>Average</b> | <b>21.37</b> | <b>23.37</b>                           |
| % change       | N/A          | 9.34                                   |

## Flash graphene in asphalt

In this project, metallurgical coke turbostratic graphene (MC-TG) has been demonstrated as a potential additive to asphalt binders to improve their aging performance. By blending 2 wt% of MC-FG in PG 67-22 asphalt binder, the aging, induced elasticity, and cracking issues are significantly reduced. In asphalt applications, air will gradually oxidize the asphalt binders and make them become rigid and less flowable. Therefore, stresses are prone to accumulate within asphalt binders, leading to the development of cracks. At the lab scale, aging of asphalt binders is studied using a Rolling Thin Film Oven (RTFO), which mimics the oxidation of an asphalt binder during processing, and a Pressure Aging Vessel (PAV), which mimics the long-term oxidation of an asphalt binder during road operations. After RTFO and 40-hour PAV tests, we found that the performance of the MC-TG-modified asphalt binder is comparable to that of the Styrene-butadiene-styrene SBS-modified binder (Figure 34), both are much superior to a neat asphalt binder. The improvement of aging performance is more clearly shown in the  $\Delta T_c$  chart (Figure 35), an indicator of the effect of aging and additives on the asphalt rheology. In the  $\Delta T_c$  chart, the region above the black line is  $\Delta T_c$ , which means the binders are too rigid to release the stress. The arrow indicates the change during aging. It is shown in the chart that all asphalt binders become rigid during the aging process, but the MC-TG modified ones have a slower rate of rigidity progression.

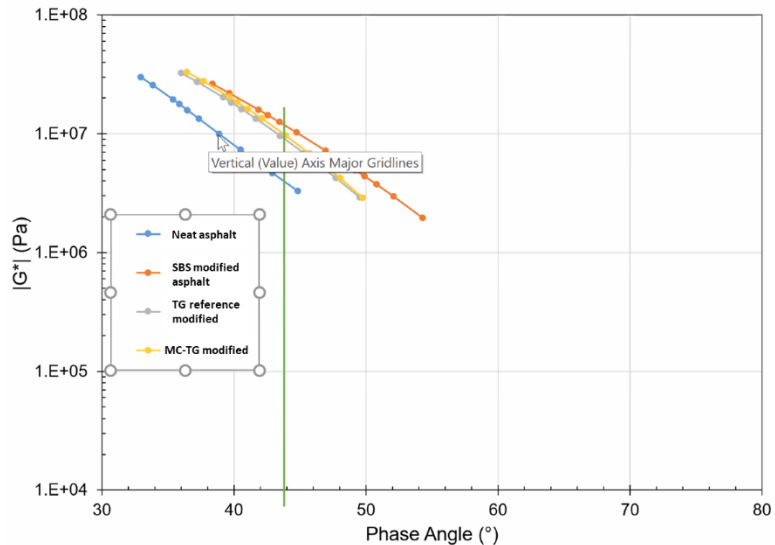


**Figure 34.** Frequency sweep tests after long-term aging (PAV) of asphalt samples

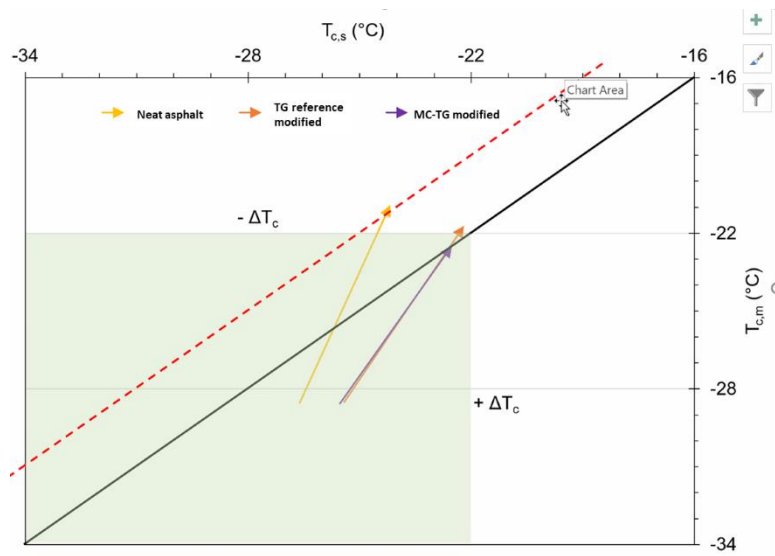


**Figure 35.**  $T_{c,s}$  -  $T_{c,m}$  aging chart for asphalt samples

MC-TG was investigated as an additive to asphalt binder to improve its aging performance. The high defect MC-FG (MC-HD) was blended into a base binder (PG 67-B) using a high shear mixer. The rheology of MC-FG modified binder was investigated as-prepared, after rolling thin film oven (RTFO) aging, and after RTFO + 40 hr. pressure aging vessel (PAV). The results were compared to that of the base binder and the SBS-modified binder (PG 76-22).

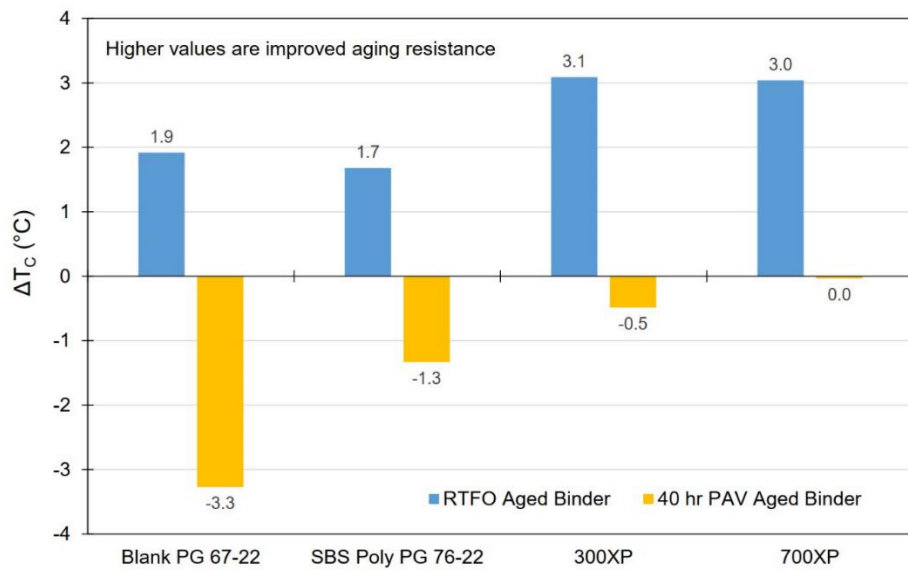
Table 3 summarizes computed  $\delta$  (Phase angle at  $G^* = 8.967$  MPa, where a larger value is better), G-R value (Rowe 2011 parameter) that indicates the rheological performance, cracking and aging susceptibility, where lower value is better), and R-value (predictor of overall fatigue strain capacity, where a lower value is better). As shown in

Table 3, the addition of MC-HD can improve the rheology of asphalt binder, especially after being aged.

**Table 3.** Rheology properties of base asphalt binder, SBS-, and MC-FG- modified binder

| Material            | Unaged   |      |         | RTFO Aged |      |         | RTFO + 40 hr PAV |       |         |
|---------------------|----------|------|---------|-----------|------|---------|------------------|-------|---------|
|                     | $\delta$ | G-R  | R-value | $\delta$  | G-R  | R-value | $\delta$         | G-R   | R-value |
| <b>67-B</b>         | 58       | 693  | 1.44    | 50.64     | 3671 | 1.72    | 39.46            | 22286 | 2.37    |
| <b>PG 76-22</b>     | 57.05    | 1497 | 1.44    | 51.08     | 4235 | 1.69    | 45.36            | 13231 | 1.99    |
| <b>0.5% - MC-HD</b> | 59.04    | 846  | 1.37    | 54.71     | 2442 | 1.51    | 40.73            | 22741 | 2.28    |
| <b>1% - MC-HD</b>   | 55.92    | 1206 | 1.48    | 51.34     | 3146 | 1.68    | 45.28            | 20431 | 1.96    |
| <b>2% - MC-HD</b>   | 57.97    | 1315 | 1.39    | 55.1      | 2925 | 1.5     | 44.06            | 18940 | 2.02    |

The age performance is also examined by calculating the  $\Delta T_c$ .  $\Delta T_c$  is widely used parameter that is associated with block cracking caused by embrittlement of the asphalt binder due to climatic effects. It is calculated by the difference between  $T_{c,s}$  and  $T_{c,m}$  that are determined using the results of bending beam rheometer (BBR, AASHTO T313) at different low temperatures. Generally, an asphalt binder is out of service when  $\Delta T_c$  is lower than -3 [14]. As shown in Figure 36, by modifying with MC-FG, the  $\Delta T_c$  of the binder is improved almost 0 after 40 hr. PAV aging, showing a tremendous improvement over the base binder (-3.3) and even SBS modified binder (-1.3). The aging performance is represented by the intersection of  $T_c$  (stiffness) and  $T_c$  (m-value) (Figure 37), which shows the MC high d modified binders are 170% better than the base binder, and almost double the performance of the SBS-modified binder.



**Figure 36.**  $\Delta T_c$  of graphene modified asphalt binder compared to base binder and SBS-modified binder

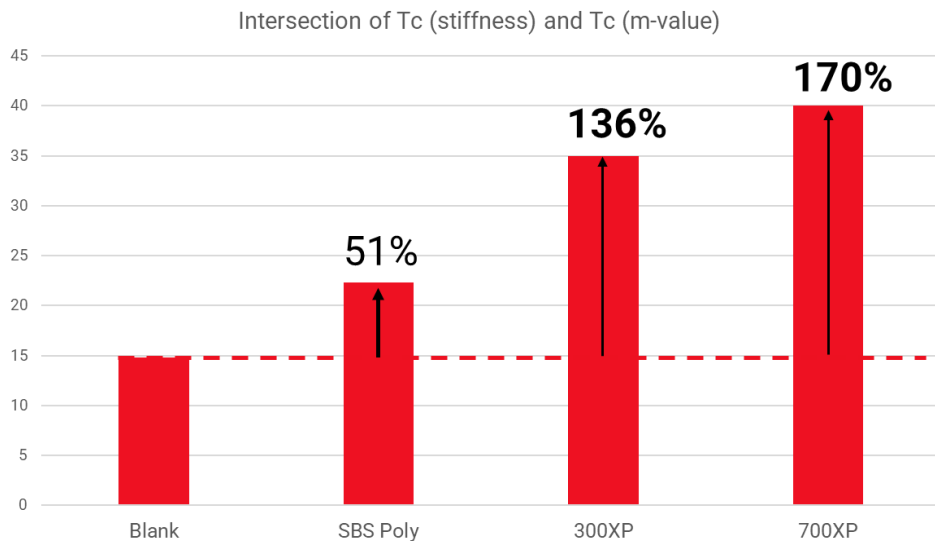


**Figure 37.** Intersection of  $T_{c,s}$  and  $T_{c,m}$  of base asphalt binder, SBS modified binder, and graphene modified binder

#### Flash graphene in epoxy/coatings

The metallurgical coke derived graphene (MC-FG) was applied to a typical epoxy coating to improve its anticorrosive performance. The MC-FG powder was first dispersed in a Bis-F epoxy using a speed mixer to yield a master batch solution of 10 wt% graphene concentration. This master batch solution was further diluted with Bis-A epoxy as the “Part A”. The resin was made with designed graphene concentrations by mixing the above Part A with Versamid 125 (“Part B”). The anticorrosive performance was examined by water permeation test. The test was performed by coating a 12 mils (~0.3 mm) film of the as-prepared epoxy resin over a shot-blasted steel. Four dollies were glued on the surface of epoxy coating. The sample was submerged in sea water at 170°F (100 psi) for 14 days and the adhesion strength was investigated by pulling off the dolly.

Three types of MC-FG, including MC-FG with medium surface area (MC-MSA), MC-FG with high surface area (MC-HSA), and chemical milled MC-FG (MC-HQ) were studied in the tests. As shown in Figure 38, all MC-FGs significantly improved the adhesion strength compared to the neat resin which contains no graphene compound, indicating a better anticorrosion performance. It is noted that the max pulling capability of the instrument is 1200 psi and all the numbers above 1200 psi in Figure 38 mean the adhesion is too strong to allow the dolly to be pulled out. For both MC-MSA and MC-HSA, a better pulling performance is observed at low concentrations (0.005 wt% and 0.01 wt%, respectively), while MC-HQ has a better and more uniform improvement at high concentrations (0.025 wt%) with none of the dollies being pulled out.

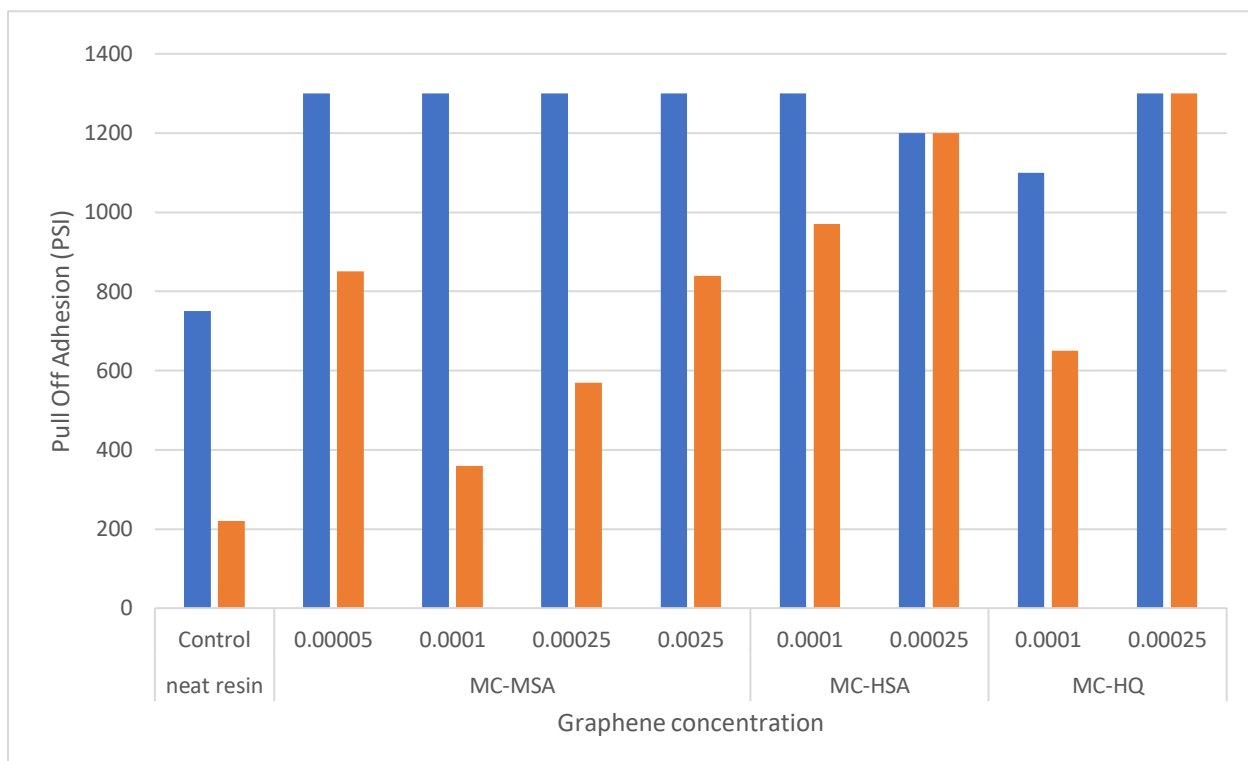


**Figure 38.** Water permeation test of MC-FG improved epoxy coating

The flash graphene (FG) obtained from the FJH of metallurgical coke (FG-MC), was studied as an additive in an epoxy composite for mechanical enhancements in collaboration with the Graphene Council. The as-flashed MC-FG was first exfoliated using a chemical-mechanical milling process as follows: The exfoliated MC-FG was first mixed into a bisphenol-F-epoxy resin masterbatch with a good homogeneity and stability. The masterbatch was then diluted by adding more of the same resin to the concentration of 0.1% and 0.5% using a high-speed orbital mixer and then was degassed under vacuum. The resin was then mixed with a stoichiometric amount of Omicure DDA 10 dicyandiamide curative, poured onto molds at 60°C and cured for 30 min. The sample was then subjected to a three-hour post-cure at 160°C. In comparison to the control sample, which has no graphene or other additives, the exfoliated MC-FG at 0.5% concentration showed a 3.1% improvement in flexural modulus, a 14.5% improvement in flexural strength, and a 25.0% improvement in flexural strain. For both flexural strength and strain, the exfoliated MC-FG has achieved the highest level of performance among the anonymous 17 total graphene samples which have been tested in this project.

#### Technoeconomic analysis

Based on our process development at the Houston Innovation Center and the design basis for our Demonstration Plant, we have developed the following economic summary of the FJH process to convert coal derived feedstocks to graphene. The summary in Table 4 demonstrates the feasibility of this process to substantially upcycle coal derived feedstocks [15].

**Table 4.** Economic summary of the Flash Joule Heating process to convert coal derived feedstocks to graphene

|                       | Demo Plant Scale<br>@ 1 shift (\$/kg) | Demo Plant Scale<br>@Full Utilization<br>(\$/kg) |
|-----------------------|---------------------------------------|--|
| <b>Variable Costs</b> | \$35.00                               | \$15.00  |
| <b>Fixed Costs</b>    | \$55.00                               | \$20.00  |
| <b>Total Costs</b>    | \$90.00                               | \$35.00  |
| <br>                  |                                       |  |
| <b>Price Range *</b>  | \$40-\$200                            | \$40-\$200                                       |

\*Based on Graphene Council 2023 Report

As noted previously, we have tested coal/metallurgical coke derived graphene in several applications including industrial coatings and lubricants. As noted in the Graphene Council Report 2023, Table 5 summarizes the graphene potential in some of these specific applications [16].

**Table 5.** Market Projects for Graphene in Coatings, Adhesive, and Lubricants

| Graphene in Coatings, Adhesives & Lubricants |                           |  |                         |                    |                                   |
|--|---------------------------|--|-------------------------|--------------------|-----------------------------------|
| Application                                  | Size of Underlying Market | Opportunity (Good, Possible, Negligible) | Addressable Market Size | Market Penetration | Market for Graphene in Five Years |
| Powder Coatings                              | \$12.5 billion            | Good                                     | \$1.2 billion           | 5%                 | \$60 million                      |
| Adhesives & Sealants                         | \$50 billion              | Possible                                 | \$1 billion             | 1%                 | \$10 million                      |
| Lubricants                                   | \$16.2 billion            | Good                                     | \$2 billion             | 5%                 | \$100 million                     |
| Thermal Management Coatings                  | \$4 billion               | Excellent                                | \$400 million           | 10%                | \$40 million                      |
| EMI Coatings                                 | \$7 billion               | Possible                                 | \$1 billion             | 1%                 | \$10 million                      |
| Anti-Corrosion                               | \$29 billion              | Excellent                                | \$12 billion            | 10%                | \$1.2 billion                     |
| Conductive Inks                              | \$2.5 billion             | Excellent                                | \$2.5 billion           | 10%                | \$250 million                     |
| Anti-Icing                                   | \$1 billion               | Excellent                                | \$1 billion             | 10%                | \$100 million                     |
| Barrier Coating                              | \$4 billion               | Possible                                 | \$500 million           | 1%                 | \$5 million                       |
| Anti-Microbial                               | \$9 billion               | Good                                     | \$1.5 billion           | 5%                 | \$75 million                      |
| <b>Total</b>                                 |                           |  |                         |                    | <b>\$1.85 billion</b>             |

Source: *The Graphene Council, The Graphene Report 2023*

## Technology Gap Assessment (TGA)

Per the technology readiness levels (TRL) definitions included in DE-FOA-0002185, the TRL of the FJH of coal at the beginning of cooperative agreement DE-FE0031988 was assessed at TRL 4. Upon completion of the project, the TRL has advanced to TRL5. The assessment (TGA) presented in Table 6 demonstrates the additional research and development (R&D) needed to scale-up or commercialize the subject technology.

**Table 6. Technology Gap Assessment**

| Gap description   | Action plan(s)  | Desired outcome   |
|---|---|---|
| Flashing containment materials cannot withstand the flashing (FJH) temperature and degrade.   | <ul style="list-style-type: none"> <li>Design of experiments (DoE) to find materials that can withstand the flashing temperature or serve as an economical sacrificial layer to protect the flashing containment.</li> <li>Design the trough (FJH reactor) to redirect the heat from the trough materials.</li> </ul> | <ul style="list-style-type: none"> <li>The best scenario is to find a material that withstands the flashing temperature and a trough design that allows rapid cooling of the trough after flash.</li> <li>A backup plan is to find a sacrificial layer material to cover/protect the trough material from the flash heating cycle.</li> </ul> |
| Feedstock selection is limited to metallurgical coke and anthracite coal.   | <ul style="list-style-type: none"> <li>Test the pre-treatment of bituminous coal and other coal feedstocks prior to FJH.</li> <li>Test the co-flash of flashable and unflashable feedstocks.</li> </ul>   | <ul style="list-style-type: none"> <li>Pre-treatment increases conductivity of the feedstock and decreases the volatile content.</li> <li>Co-flash could remove the need for pre-treatment.</li> </ul>  |
| Coal derived FG cannot be readily dispersed in solution. For now, chemical assisted exfoliation is the leading method for dispersing coal derived FG. | <ul style="list-style-type: none"> <li>Testing different exfoliation methods such as liquid phase exfoliation and different methods of milling.</li> <li>DoE to find the flashing parameters or coal feedstock that produces FG that is easier to disperse.</li> </ul>  | <ul style="list-style-type: none"> <li>Choose an exfoliation method that effectively exfoliates and disperses the FG. The economics of the method should be less than \$10/kg.</li> <li>Choose a consistent feedstock supply with optimized flashing parameters for the exfoliation.</li> </ul>   |
| Many applications for coal derived flash graphene (FG) have been demonstrated. The results need to be elaborated to industrial testing.               | <ul style="list-style-type: none"> <li>Work with partners or customers with industrial standards to repeat the improvement results.</li> </ul>  | <ul style="list-style-type: none"> <li>Select one leading application for the first graphene product.</li> </ul>  |
| Gap to reach TRL6 - Not yet demonstrated effective flashing of coal derived feedstocks in an operational  | <ul style="list-style-type: none"> <li>Demonstration Plant is expected to commence operations during 4Q2023. Once the plant and process are stabilized (~2Q2024), we will evaluate coal</li> </ul>  | <ul style="list-style-type: none"> <li>Confirm coal derived feedstocks can be effectively converted to graphene at the scale of the Demo Plant (~1t/day).</li> </ul>  |

|                                 |   |  |
|---------------------------------|---|--|
| environment (e.g., Demo Plant). | derived feedstocks in this environment. |  |
|---------------------------------|---|--|

## Bibliography and References

- [1] T. Puiu, "The 'Wonder Material': How Graphene Is Set to Change the World," *Lindau Nobel Laureate Meetings*, 27 03 2019.
- [2] K. I. Bolotin, K. J. Sikes, Z. Jiang, M. Klima, G. Fudenberg, J. Hone, P. Kim and H. L. Stormer, "Ultrahigh electron mobility in suspended graphene," *Solid State Commun.*, vol. 146, no. 9, p. 351, 2008.
- [3] A. A. Balandin, S. Ghosh, W. Bao, I. Calizo, D. Teweldebrhan, F. Miao and C. N. Lau, "Superior thermal conductivity of single-layer graphene.," *Nano Lett.*, vol. 8, no. 3, p. 902, 2008.
- [4] J. S. Bunch, S. S. Verbridge, J. S. Alden, A. M. van der Zande, J. M. Parpia, H. G. Craighead and P. L. McEuen, "Impermeable atomic membranes from graphene sheets.," *Nano Lett.*, vol. 8, no. 8, p. 2458.
- [5] X. Du, I. Skachko, A. Barker and E. Y. Andrei, "Approaching ballistic transport in suspended graphene.," *Nat. Nanotechnol.*, vol. 3, no. 8, p. 491, 2008.,
- [6] A. H. Castro Neto, F. Guinea, N. M. R. Peres, K. S. Novoselov and A. K. Geim, "The electronic properties of graphene.," *Rev. Mod. Phys.*, vol. 81, no. 1, p. 109, 2009.
- [7] R. R. Nair, P. Blake, A. N. Grigorenko, K. S. Novoselov, T. J. Booth, T. Stauber, N. M. R. Peres and A. K. Geim, "Fine structure constant defines visual transparency of graphene.," *Science*, vol. 320, no. 5881, p. 1308, 2008.
- [8] C. Lee, X. Wei, J. W. Kysar and J. Hone, "Measurement of the elastic properties and intrinsic strength of monolayer graphene," *Science*, vol. 321, no. 5887, p. 385, 2008.
- [9] A. P. Kauling, A. T. Seefeldt, D. P. Pisoni, R. C. Pradeep and R. Bentini, "The worldwide graphene flake production.," *Adv. Mater.*, vol. 30, no. 44, p. 1803784, 2018.
- [10] "Conversion of Domestic US Coal into Exceedingly High-Quality Graphene.," William Marsh Rice University, Houston, TX, 2022.
- [11] D. Luong, K. Bets and W. e. a. Algozeeb, "Gram-scale bottom-up flash graphene synthesis," *Nature*, vol. 577 , no. 7792, p. 647, 2020.
- [12] U. E. I. Administration, "GLOSSARY," Washington, DC.
- [13] U. E. I. Administration, "Coal prices and outlook," Washington, DC, 2022.

[14] Petersen, J. Claine. "A review of the fundamentals of asphalt oxidation: chemical, physicochemical, physical property, and durability relationships." *Transportation research circular E-C140* (2009).

[15] Graphene Council Report 2023

[16] Graphene Council Report 2023